UNCLASSIFIED

AD NUMBER:	AD0477749

LIMITATION CHANGES

TO:

Approved for public release; distribution is unlimited.

FROM:

Distribution authorized to U.S. Government agencies and their contractors; Export Controlled; 1 Nov 1965. Other requests shall be referred to Air Force Flight Dynamics Laboratory, Wright-Patterson AFB, OH 45433.

AUTHORITY

AFFDL ltr dtd 24 Jan 1973

THIS PAGE IS UNCLASSIFIED

AFFDL-TR-65-130

477749
19

DESIGN AND COMPENSATING TECHNIQUES INVESTIGATION FOR HIGH TEMPERATURE OPERATION OF P-SILICON PRESSURE TRANSDUCER

FRANK L. YUAN

SCHAEVITZ-BYTREX, INC.
WALTHAM, MASSACHUSETTS

TECHNICAL REPORT AFFDL-TR-65-130

NOVEMBER 1965

DDC
FEB 21 1966
TISIA E

This document is subject to special export controls and each transmittal to foreign nationals may be made only with prior approval of the Flight Control Division (FDC), Air Force Flight Dynamics Laboratory, Wright-Patterson AFB, Ohio.

AF FLIGHT DYNAMICS LABORATORY
RESEARCH AND TECHNOLOGY DIVISION
AIR FORCE SYSTEMS COMMAND
WRIGHT-PATTERSON AIR FORCE BASE, OHIO

NOTICES

When Government drawings, specifications, or other data are used for any purpose other than in connection with a definitely related Government procurement operation, the United States Government thereby incurs no responsibility nor any obligation whatsoever; and the fact that the Government may have formulated, furnished, or in any way supplied the said drawings, specifications, or other data, is not to be regarded by implication or otherwise as in any manner licensing the holder or any other person or corporation, or conveying any rights or permission to manufacture, use, or sell any patented invention that may in any way be related thereto.

Copies of this report should not be returned to the Research and Technology Division unless return is required by security considerations, contractual obligations, or notice on a specific document.

100 - January 1966 - 27-516-773

DESIGN AND COMPENSATING TECHNIQUES INVESTIGATION FOR HIGH TEMPERATURE OPERATION OF P-SILICON PRESSURE TRANSDUCER

FRANK L. YUAN

SCHAEVITZ-BYTREX, INC.
WALTHAM, MASSACHUSETTS

This document is subject to special export controls and each transmittal to foreign nationals may be made only with prior approval of the Flight Control Division (FDC), Air Force Flight Dynamics Laboratory, Wright-Patterson AFB, Ohio.

FOREWORD

Contract No. AF33(615)-1865

Project No. 8224

Task No: 822403

Prime Contractor: Schaevitz-Bytrex, Inc.
223 Crescent Street
Waltham, Massachusetts

Subcontractor: Kulite Semiconductor Products, Inc.
1030 Hoyt Avenue
Ridgefield, New Jersey

Schaevitz-Bytrex Job No: 1775

Air Force Program Monitor: J. V. Roberts, FDCL

This report covers experimental work performed between 15 July 1964 and 29 March 1965. The manuscript released May 1965 by the author for publication as an R and D Technical Report.

Major contributors to this development program are:

(1) Dr. A. D. Kurtz, Director of Research and Development
Kulite Semiconductor Products, Inc.

(2) Malcolm Green, Technical Director
Schaevitz-Bytrex, Inc.

(3) Charles Gravel, Supervisor of Semiconductor Research
Kulite Semiconductor Products, Inc.

(4) James Welsh, Project Engineer
Schaevitz-Bytrex, Inc.

This report has been reviewed and is approved.

FOR THE COMMANDER:

H. W. BASHAM
Chief, Control Elements Branch
Flight Control Division
AF Flight Dynamics Laboratory

ABSTRACT

Theoretical study and experimental work indicate that a p-n junction type diffused semiconductor sensor is not feasible for high temperature operations above 600° or 700° F. The generation of electron-hole pairs destroys the isolation property of the p-n junction. Consequently, the emphasis of the work shifted to the development of a semiconductor pressure transducer with bonded strain sensors. The bulk resistivity of the silicon sensor was established together with the technique of making a high temperature ohmic contact. A rather broad evaluation of the substrate materials was made before the final selection of special tungsten alloy for actual pressure transducer construction. Prototype transducers were built and tested at temperatures over 1000° F. The data from the temperature compensation experiments showed that the techniques and the choice of material potentially will make high temperature transducers which satisfy all the requirements of the Statement of Work for this Contract.

TABLE OF CONTENTS

PAGE

I. Introduction 1

II. P-N Junction Investigation 2

1. Fabrication of Diffused Beam Sensor 2

2. Measurement of Resistance and Junction Isolation Versus Temperature 3

3. Conclusion 5

III. Semiconductor Sensor Fabrication 6

1. Silicon Crystal Resistivity 6

2. Fabrication of Silicon Filaments 7

3. Lead Attachment 9

IV. Substrate Material Selection 11

1. Properties of Materials 11

2. Test Results 12

a. Low Expansion Alloys and Stainless Steel 12

b. Ceramics 13

c. Oxidized Silicon Substrate 14

d. Pure Tungsten 14

e. Tungsten Alloys 14

V. Strain Transmission Experiments 16

1. Bonding Agents 16

a. Ceramic Cement 16

b. Pyroceram Brand Cement #45 16

c. Brazing of Gages 18

d. Flame Sprayed Gages 18

2. Test Equipment for Strain Transmission 19

3. Test Results 19

a. Tungsten Beams 20

b. NiSpan C Beams 20

c. Silicon Beams 21

d. Ceramic Beams 22

TABLE OF CONTENTS (Cont'd)

PAGE

VI. Transducer Design 23
1. Diaphragm With Shear Beam Element 23
2. Embedded Gage Construction 24
3. Gage Diaphragm Transducers 24
VII. Pressure Transducer Evaluation 26
1. Test Equipment 26
2. Test Results 26
a. First Prototype Transducer 26
b. Second Group of Prototypes 28
c. Third Group of Prototypes 29

ILLUSTRATIONS

FIGURE		PAGE
1.	Diffused Sensor	31
2.	Sensor Isolation	32
3.	Sensor Resistance vs Temperature	33
4.	Sensor Resistance vs Temperature	34
5.	Resistivity of Silicon at 300°F as a Function of Acceptor Concentration (p-Type)	35
6.	Sensor Resistance vs Temperature	36
7.	Sensor Resistance vs Temperature	37
8.	Sensor Resistance vs Temperature	38
9.	Thermal Expansion of Various Materials	39
10.	Elevated Temperature Beam Test Setup	40
11.	Apparent Strain and Force Output vs Temperature	41
12.	Shear Beam Transducer Assembly	42
13.	Embedded Gage Type Pressure Transducer Assembly	43
14.	Gage Diaphragm Transducer Assembly	44
15.	Schematic of Pressure Test Setup	45
16.	Gage Diaphragm Type Transducer Construction	46
17.	Transducer Output at 1000 psi vs Temperature	47
18.	Transducer Output at 1000 psi vs Temperature	48

TABLES

TABLE PAGE

1. Diffused Sensor Characteristics 49
2. Thermal Generation of Carriers 49
3. Temperature Limitation for Extrinsic Behavior 49
4. Prestrain in Gages Bonded to Ceramic Materials 50
5. Gage and Isolation Resistances at Various Temperatures 51
6. Prestrain in Gages Bonded to Tungsten Alloys 51
7. Behavior of Tungsten Beam at Various Temperatures . . 52
8. Behavior of NiSpan C Beam at Various Temperatures . . 52
9. Prestrain in Gages Bonded to NiSpan C Beam 52
10. Behavior of Silicon Beam at Various Temperatures . . . 53
11. Behavior of Ceramic Beams at Various Temperatures . 53
12. Output Characteristics of Standard Pressure Transducer 54
13. Pressure Loading at High Temperatures of First Prototype 55
14. Pressure Loading at Room Temperature of Second Prototype 56
15. Pressure Loading at 227°F of Second Prototype 56
16. Pressure Loading at 548°F of Second Prototype 57
17. Pressure Loading at 235°F of Second Prototype 57
18. Pressure Loading at Various Temperatures of Third Prototype 58

SECTION I

INTRODUCTION

The propulsion engines of the new aerospace age operate at ever increasing temperature. To aid in developing these engines and evaluating their performance, there must be transducers capable of making accurate measurements at high temperatures.

Some of the most accurate transducers in use today for making measurements at temperatures below 400°F are of the strain gage type. However, the strain gages typically used in these devices have not been satisfactory for continued service at temperatures up to 600°C.

The discovery of the strain sensitive properties of semiconductor materials offered promise of strain gage transducers for elevated temperature operation. Because of their higher signal outputs which are not attenuated to impractical levels at elevated temperatures and their resistance to oxidation, semiconductor strain gage devices offer many theorectical advantages.

This program was undertaken to attempt to realize these advantages in a practical pressure transducer for general purpose use at 600°C.

SECTION II

P-N JUNCTION INVESTIGATION

The fabrication of a semiconductor strain gage circuit can be achieved by the use of diffused p-n junctions obtained by the process of solid state diffusion and associated solid state technology. This process was investigated because of the following distinct advantages.

a. The strain sensitive members are atomically bonded to the load-bearing members.

b. Desired resistances, from ohms to megohms, can be achieved independently of the bulk geometry.

c. The location and configuration of the active regions are subject to more exacting control than other known methods.

d. The electromechanical and thermal properties of the active region can be tailored to fit a wide range of specific requirements.

Diffused beam sensors in silicon were fabricated. Measurements of sensor isolation from the substrate material as a function of temperature indicate that at 400°C the p-n junction resistance has decreased to approximately 40K ohms from an isolation of 5 megohms at room temperature. Theorectical calculations are presented to show that thermal generation of hole-electron pairs is responsible for the degradation of the isolation resistance, and that this mechanism rules out the use of silicon for diffused transducers to operate in a 300-600°C temperature range.

1. FABRICATION OF DIFFUSED BEAM SENSORS

Diffused beam sensors were fabricated using n-type silicon of resistivity 5 ohm-centimeter as the starting material. A S_iO_2 layer obtained by oxidizing the silicon at 1000°C for 1 hour in steam provided a selective mask against the diffusion of boron which formed the strain sensing elements. This oxide layer was approximately 5000A° thick. Selective areas of the S_iO_2 were removed by photolithographic techniques to define the sensor geometry (see Fig. 1).

Kodak Photosensitive Resist (KPR) exposed to ultra-violet light through a negative film mask of the desired sensor pattern is the basis of the photolithographic process. The exposed KPR hardens into a protective film against subsequent oxide etching, whereas the masked KPR is removed in a developing solution.

The diffused sensors were made using a two-step diffusion process to form p-type regions in the pattern areas from which the S_iO_2 has been removed. The vapor of boron trioxide was passed over the silicon heated to 900°C for 45 minutes using dry nitrogen as the carrier gas. After this predeposition step the vapor source was removed and the temperature of the silicon increased to 1100°C to allow solid state diffusion to proceed

for one hour in air. Diffused layer sheet resistivities of 5 to 6 ohms per square were obtained with this process. Measurements made on a typical diffusion run are shown on Table 1.

The contact areas of the sensors were plated using electroless nickel followed by an electroplated gold strike.

The finished beam consisted of two planar diffused p-type strain gages on bulk n-type silicon. The p-n junctions were surface passivated in the sense that all junction interfaces at the surface are protected from the environment by the thermally grown silicon dioxide layers.

2. MEASUREMENTS OF RESISTANCE AND JUNCTION ISOLATION VERSUS TEMPERATURE

The sensor resistance and sensor isolation from the substrate material were measured as a function of temperature from room temperature to approximately 200°C. Resistance measurements were made using a Wheatstone Bridge (Industrial Instruments Model RN-1) and temperature was contolled and measured using a Bytrex Temperature Control Unit (Schematic Model No. 126W3-V).

Fig. 2 is a plot of the junction isolation resistance of four sensors versus the reciprocal of the absolute temperature. This plot is representative of the degradation of junction isolation with temperature of diffused silicon sensors. At 25°C, sensor isolation from the substrate of 4 megohms or greater, measured at 1 volt, is easily obtained. Junction isolation is essentially the resistance of a reverse biased p-n junction through which a low-level saturation current flows. The saturation current is reasonably independent of the applied reverse voltage over a designable voltage range and up to the breakdown voltage of the p-n junction. Thus, the junction isolation resistance is a linearly increasing function of the reverse voltage until breakdown occurs, assuming the reverse current has no large, additional components such as surface leakage. The isolation resistance plotted in Fig. 2 is the resistance between sensors as measured on a Wheatstone bridge. The voltage across the p-n junction would be something less than 1 volt in this case. The reverse current flowing is of the order of 10^{-7} amperes.

Figs. 3 and 4 show the resistance changes of the same sensors over this temperature range. The sensor isolation decreases rapidly with increasing temperature, having the electrical effect of a shunting resistance path across the diffused strain gage resistor. As the lowering shunt resistance approaches the resistance of the sensor, the resistance measured experimentally is materially affected by the shunting path. This is shown in Fig. 4 for the two sensors with lower isolation selected to illustrate the effect. The measured resistance goes through a maximum with temperature as the shunting path due to the decreasing junction isolation begins to dominate the parallel combination, then decreases as the shunting resistance takes over.

At 180°-200°C the isolation is on the order of 10K ohms for the better isolated sensors, and an extapolation to the 300°-400°C temperature range shows that there would be very little isolation in this range. This behavior is a result of the temperature dependence of the junction saturation current. The saturation current is a flow of electrons and holes, minority carriers in the regions from which they come, across the junction boundary. As the silicon is heated an increasing number of electrons are raised into the conduction band by the thermal energy acquired, there by creating more minority carriers on each side of the junction which contribute to an increasing saturation current. The ability of the junction to isolate the diffused sensor is degraded because of the increase of this intrinsic conduction component with temperature. The saturation current density is proportional to the square of the number of carriers in intrinsic silicon, or the number of thermally generated hole-electron pairs.

$$n_i^2 = 1.5 \times 10^{33} \times T \times \exp\left(-\frac{14028}{T}\right) \text{ cm}^{-6}$$

Thermal generation of carriers is illustrated in Table 2.

At approximately 400°C the saturation current will have increased by 13 orders of magnitude and at 200°C by 9 orders of magnitude due to the thermal generation of electron-hole pairs.

The saturation current density is given by

$$J_s = \frac{kT}{q} \cdot \frac{b}{(1+b)^2} \cdot \sigma_i^2 \cdot \frac{1}{\sigma_n L_p}$$

where $b = \frac{\mu_n}{\mu_p}$ = ratio of electron to hole mobility

$\sigma = q\, n_i \cdot (\mu_n + \mu_p)$

$L_p = \sqrt{D_p \tau}$ = hole diffusion length equal to about 6×10^{-3} cm in silicon having a carrier lifetime of 1 microsecond

L_n = hole diffusion length, approx. 3×10^{-3} cm

σ_n = conductivity of bulk silicon = 2.2×10^{-1} (ohm-cm)$^{-1}$

At room temperature a calculation using the appropriate constants for silicon indicates that $J_s \lessapprox 10^{-10}$ amp/cm. The diffused sensors have a junction area of 1.5×10^{-3} cm^2, therefore at room temperature the saturation current due to thermal pair-generation is

$$I_s = 10^{-10} \times 1.5 \times 10^{-3} \text{ amps} = 1.5 \times 10^{-13} \text{ amps}$$

The sensors actually are passing about 10^{-7} amperes at room temperature (as indicated by a junction resistance of 5 megohms at 1 volt reverse bias) in which range the current is dominated by junction leakage components.

However, the leakage components vary only linearly with temperature whereas the intrinsic conduction caused by thermal generation of hole-electron pairs has an exponential dependence on temperature. As tabulated above, at 200°C the intrinsic conduction has increased by 10^9 times, or from the calculated value of 10^{-13} amperes to 10^{-4} amperes. Thus, the junction current is now determined to a large extent by the component of intrinsic conduction. From these considerations a junction resistance of $\frac{1 \text{ volt}}{10^{-4} \text{ amp}}$ = 10K ohms is to be expected at 200°C. Fig. 1 shows that the better diffused sensors have a resistance of 10K ohms at 200°C which indicates the linear leakage component of the current is rapidly being overtaken by the exponential intrinsic component.

At 400°C the calculated intrinsic conduction has increased by 10^{13} times, thus the saturation current has increased from a room temperature value of 10^{-13} amperes to 1 ampere at 400°C. An extrapolation of Fig. 2 to 400°C confirms the calculation and it is clear that the sensor isolation from the substrate material is vanishing at this temperature.

3. CONCLUSIONS

a. Diffused silicon sensors are useful for transducers designed to about 300°C.

b. At temperatures greater than 400°C thermal generation of hole-electron pairs removes completely the isolation capability of p-n junctions in silicon diffused sensors.

c. The best choice for the temperature range to 600°C is a structure wherein the silicon sensor is electrically separated from the structural member of the transducer, and its characteristics are independent of p-n junction isolation requirements.

SECTION III

SEMICONDUCTOR SENSOR FABRICATION

Due to the temperature limitation of the diffused junction devices, investigation proceeded along the line of obtaining piezoresistive properties of silicon by attaching gages to stressed member of a transducer. High temperature behavior of three p-type silicon resistivities was investigated together with lead attachment techniques.

1. SILICON CRYSTAL RESISTIVITY

In silicon, as in any other semiconductor, current is carried by free holes and electrons. There are two fundamental ways to produce these free carriers inside the bulk of the crystal:

a. Addition of doping impurities during the growth of the crystal. At low temperatures the conductivity of silicon depends very sensitively upon the impurity content. Impurity conductivity is usually referred to as extrinsic conductivity.

b. The creation of hole-electron pairs inside the crystal lattice by rupturing the bonding electrons of silicon atoms. The rupturing action can be caused by heat; the thermal generation of hole-electron pairs. This type of conductivity is usually referred to as intrinsic conductivity. At sufficiently high temperature all silicon approaches a common conductivity behavior given by the intrinsic conductivity. The activation energy for hole-electron pair production is equal to the energy gap of the material and by Maxwell-Boltzmann statistics the number of carriers in intrinsic material increases exponentially with temperature

$$n_i^2 = AT^3 \exp\left(-\frac{E_g}{kT}\right)$$

Thus, the increase in conductivity is rapid when the intrinsic conductivity range is approached.

The selection of the best doping level to minimize temperature effects must take into consideration other desirable characteristics, such as sensor resistance and transducer output signal level. Since the temperature behavior of the conductivity of silicon reverses direction in passing from extrinsic to intrinsic conductivity domination, it is desirable to select an impurity doping level that will insure extrinsic conductivity over the temperature range to 600°C for this transducer application. In general, higher doping levels extend the extrinsic conductivity range. When the number of thermally generated hole-electron pairs in silicon,

$$n_i^2 = \left[1.5 \times 10^{33} \times T^3 \times \exp\left(-\frac{14028}{T}\right) cm^{-6}\right]^{1/2}$$

(where is in degrees Kelvin) approaches the impurity doping concentration, the temperature coefficient of resistance reverses from positive to negative values. At a temperature of 600°C,

$$n_i = 3.3 \times 10^{17} \ cm^{-3}$$

Therefore, an impurity doping level an order of magnitude larger, or even more, than 10^{17} cm^{-3} is indicated for extrinsic conductivity behavior to 600°C. Fig. 5 is a plot of room temperature resistivity of p-type silicon versus impurity concentration for the doping range of interest, and it is seen that an impurity concentration of 3.3×10^{17} cm^{-3} corresponds to a resistivity of 0.13 ohm-centimeter. For impurity concentration an order of magnitude greater, 3×10^{18} cm^{-3}, the resistivity is 0.03 ohm-cm and for two orders of magnitude greater, 10^{19} cm^{-3}, a resistivity of 0.01 ohm-cm is indicated.

High temperature behavior of the three resistivities 0.1, 0.03, and 0.01 ohm-centimeter was measured in conjunction with the study of high temperature contacts to p-type silicon. Figs. 6, 7 and 8 are plots of sensor resistances, normalized to room temperature, against temperature. The approximate temperatures at which extrinsic conductivity behavior of the sensors remains predominant are shown on Table 3.

These experiments were made using a wire-wound tube-type furnace capable of temperature to 1200°C. The sensor leads were welded to .020" diameter platinum wire which extended to the terminals of an Industrial instruments Model RN-1 Wheatstone Bridge. The sensor temperature was measured by a chromel-alumel thermocouple placed as close to the sensor as possible. It is felt that the spread in the data taken is caused almost entirely by temperature differentials between the thermocouple and the sensor due to the physical separation and temperature gradients within the furnace.

We concluded from these measurements that a resistivity of .01 ohm-cm is the highest resistivity of p-type silicon that remains extrinsic to 600°C, and selected it for further work.

2. FABRICATION OF SILICON FILAMENTS

A considerable amount of preparation of the silicon is necessary to insure against metal-semiconductor rectification. The basic idea is to make the contact area for later lead attachment the most highly doped silicon surface attainable. Due to the various approaches in lead attachment, the crystal is prepared differently.

(1) For bonding or welding: The following process for making the 0.01 ohm-centimeter p-type silicon sensor using silver-gallium contacts has been developed and tested extensively with excellent results:

(a) Silicon ingot of resistivity .01 ohm-centimeter p-type crystallographically oriented for slicing parallel to the (110) plant, and 111 direction in this plane.

(b) Slice silicon ingot into .012" slices.

(c) Lap slices to .006" thickness.

(d) Clean slices thoroughly in hot alconox solution, rinse in trichlorethylene. Treat in nitric acid prior to diffusion.

(e) Coat both surfaces of slices with solution consisting of 2 grams of Boracic Acid dissolved in 35 cubic centimeters of ethylene glycol monomethyl ether.

(f) Diffuse at 1175°C for 17 hours in air.

(g) Cut rectangles 0.150" wide, oriented for $\langle 111 \rangle$ direction across width.

(h) Remove borosilicate glassy layer acquired during diffusion from one side of rectangle by etching in hydrofluoric acid.

(i) Remove borosilicate glassy layer from a centered stripe .050" wide on other side of rectangle, using apiezon wax to mask portion of glassy layer not removed.

(j) Dice rectangles in filaments measuring .150" x .010" x .006", with $\langle 111 \rangle$ crystallographic direction along length.

(k) Wax contact ends of filaments. Etch in etch composition of 8 parts nitric acid, 2 parts hydrofluoric acid for 45 seconds. Remove wax and place filaments in hydrofluoric acid for two minutes. Rinse well in demineralized water.

(2) The silicon is prepared for nickel plating in the same manner as was described above for silver bonded contacts. A heavily doped, diffused p-type layer is necessary for low contact resistance and the nickel plate is applied after the diffusion process. Immediately prior to plating, the wafers are dipped in hydrofluoric acid to remove any oxide present and rinsed in demineralized water. The wafers are immersed for 3 minutes in the plating bath maintained at a temperature of 95°C, then annealed at 830°C for 10 minutes in dry Forming Gas (85% N_2, 15% H_2). The silicon is replated in the nickel bath for 3 minutes after annealing. The resulting nickel surface can be soldered readily with standard soft solder methods, and may be electroplated with gold and other metals for protection of the nickel.

(3) Electroless silver plating to silicon was investigated, but the adherence of the plate is poor. This technique is not considered reliable for low resistance ohmic contacts without further extensive investigation. Because of the promise of the silver bonded and nickel-plated contacts, we did not pursue the electroless silver plating technique beyond a few trials. It is believed that the large difference between the thermal expansion coefficient of the two materials could be responsible for the poor adherence.

3. LEAD ATTACHMENT

Two approaches were investigated for attaching leads to the silicon filament. They are:

(1) Bonding, or welding, gallium-doped silver wire. Silver-gallium (1%) wire of .003" diameter was attached to the ends of the filament described previously by a modified welding technique which alloys the wire to the silicon. Both current and pressure were applied in order to alloy the wire to the silicon. The final resistance of the filament was obtained by masking the contact with apiezon wax and etching the silicon in hydrofluoric nitric acid compositions.

These sensors were measured from room temperature to 700°C, Fig. 6, and rectification does not appear to be a problem. Occasionally a silver-gallium bonded sensor will be found to have rectifying contacts, but this is not a function of temperature. Such a sensor will rectify at room temperature and is rejected immediately. The cause of rectification is thought to be associated with the penetration of the bond and the recrystallization conditions during the bonding operation. A sensor that does not rectify at room temperature does not rectify at increasing or decreasing temperatures.

During the later stages of the contract, due to the chemical attack on the gallium-doped silver wire by some bonding cement after prolonged exposure to high temperature, both pure platinum and boron-doped silver wires were employed. While a marked reduction on the rate of attack was observed on the boron-doped silver wire, there was no sign of attack shown by the platinum wire. Both of the new wires were bonded to the silicon with basically the same technique described above with some variations in the critical settings.

Other methods such as electroless nickel and silver plating were also investigated for the high temperature ohmic contacts, but we consider the bonding or welding technique a more suitable approach for transducer application.

(2) Electroless nickel and silver plating. Silver leads were attached to the filament by using Hanovia Silver Paste #521 which is a viscous suspension of finely divided precipitated or flaked silver in an organic vehicle. Other metallizing and brazing materials obtained and being used are Hanovia Liquid Silver #228, Eutec-Silweld 1618, Silvaloy #45, Silvaloy #60, and Easy-Flow #6040. The Liquid Silver is fundamentally the same as Silver Paste #521, and the others are high silver content brazing alloys. Optimum firing cycles have been developed for these brazing materials using a Hoskins tube-type electric furnace. One was used to attach silver leads with Silver Paste #521 to the nickel-plated contact areas of the 0.1 ohm-cm sensors measured for the curve presented in Fig. 8. The main drawback of this technique, as revealed by later results, is that the contact would invariable become noisy after exposure to high temperature for longer duration.

SECTION IV

SUBSTRATE MATERIAL SELECTION

Metallic, semiconductor and ceramic substrate materials have been tested. Two specially designed tungsten alloys have been tested and proved to be best suited for high temperature semiconductor construction. Successful gage application on ceramics and silicon test beams have been achieved, but the use of ceramics as well as silicon involves a high degree of complexity in fabrication and assembly.

1. PROPERTIES OF MATERIALS

The choice of materials feasible for semiconductor high temperature transducer construction is greatly reduced by the fact that the silicon strain sensors have an extremely low coefficient of thermal expansion. Other critical selection criteria include the favorable elastic properties at high temperatures, the ease of fabrication and assembly and the resistance to corrosion and oxidation. These criterial will be discussed separately below:

a. Thermal expansion: Prior to award of the contract, an attempt was made to bond semiconductor strain gages to low-expansion steel load-carrying elements to manufacture high-temperature transducers. These experiments were unsuccessful because the gages invariable broke as the specimens werecooled down from the cement curing temperature. This was attributed to the large differential expansion between the crystal and the steel. The coefficient of silicon is approximately 2.3×10^{-6} inches/inch per ^{o}F. The low expansion alloys such as Kovar, Rodar, and NiSpan C, available on the market, are limited to approximately 700°F before they expand rapidly with increasing temperature. Fig. 9 shows the thermal expansion data of some typical materials tested under this contract. Because of this consideration, the substrate materials are limited to silicon, tungsten, glass, and ceramics.

b. Elastic properties at high temperatures: The principle of operation of any transducer employing strain gages is based on the fact that the electrical resistance of the gage changes when a strain is applied to the gage either directly or transmitted through a bonding agent. The unbonded transducers are fragile and not as reliable as the bonded type. On the bonded transducers, the force-carrying member is subjected to a high stress level so that the strain transmitted to the semiconductor gage is relatively high as compared to the thermally induced apparent strain. Generally speaking, the minimum stress due to pressure is around 20,000 psi for the desired output level. (Proportionally lower for lower values of Young's modulus.) In order to minimize creep, hysteresis, and zero shift, the rule of thumb in transducer design is that the operating or working stress should not exceed one-third of the yield strength of the material at all temperatures. Consequently, the material selected should have a yield strength of 60,000 psi at the maximum operating temperature. This requirement eliminated many glasses and ceramics.

c. The ease of fabrication and assembly: During this contract some ceramics, as well as silicon bulk crystals, were tested for force-carrying members. Although the results were encouraging, eventually they were discontinued from further evaluation because of the difficulties in fabrication into desired geometrical shapes. Some materials can be fabricated into transducer element shapes, but the long delivery requirement does not meet the scheduling of this contract. Problems in the assembly of silicon and ceramics were also anticipated. The difficulty in design lies in the fact that the element must be assembled with the case and the diaphragm of the transducer. Because of other considerations, such as oxidation, strength and the complexity in fabrication, these brittle ceramics or silicon are not suitable for the case or diaphragm. If the case or diaphragm material is made with dissimilar material from the element, major difficulties are invariably introduced in the matching of thermal expansion coefficients. Any mismatch of the coefficients would result in additional error in the output of the transducer. Furthermore, most materials with low thermal expansion coefficient and suitable for the diaphragm and case usually are satisfactory for the element. These considerations, together with the later discovery of the feasibility of some specially made tungsten alloys, ceramic and silicon element investigation were discontinued even though successful strain transmission data had been obtained.

d. Resistance to corrosion and oxidation: Corrosion and oxidation of the material must be minimized in order to keep the sensitivity of the transducer stable over the span of 60 operating hours as required by the work statement of this contract. The tungsten alloys finally chosen for this work showed some oxidation at elevated temperatures, but external nickel plating reduced the rate considerably.

2. TEST RESULTS

A summary of the test results are tabulated below. The gages were bonded to various substrate materials by different bonding agents such as ceramic cements, silver brazing alloys, and pyroceram. These bonding agents will be discussed separately in the next section. Although the test results on different substrate materials vary slightly with the bonding agent, they do show that some substrates are more desirable than others where the gages broke upon cooling to room temperature after the bonding agent solidified.

a. Low expansion alloys and stainless steel: Several samples of NiSpan C and 17-4PH stainless steel were gaged with ceramic cements. The combination of these materials with the silicon gage was unsuccessful in the sense that the gages shattered either during cooling to room temperature from the curing temperature, or subsequent heating to 600°F or slightly higher.

One sample of Kovar was tested up to 1015°F. Although the gages were not broken during testing, the material oxidized so severely that the ceramic

cement peeled off the substrate with the gages still imbedded in the cement. All of the materials in this group were discarded from further testing.

b. Ceramics: Strain gages were brazed to several types of ceramics and beams were prepared for tests of strain transmission at room and elevated temperatures. The ceramic element technique has some significant advantages in the construction of high temperature transducers using semiconductor strain gages.

(1) Ceramics are excellent electrical insulators even at elevated temperatures.

(2) Ceramics match the expansion coefficients of semiconductor strain gages.

(3) Many ceramics are good elastic materials.

(4) The techniques may be usable at higher temperatures.

The following disadvantages should be noted when considering ceramics as load-carrying members in transducers:

(1) They are brittle and subject to damage from shock.

(2) They have a high modulus which necessitates operation at high stress levels to obtain high signals.

(3) They are difficult to fabricate and join to other materials.

(4) Some bonding agents do not adhere to them well enough for strain measurement work.

Six types of ceramics have been tested. The results showed that the thermal expansion match between the ceramics and silicon are close enough so that no gage breakage was observed. Of the six types, three were gaged with silver brazing compound and the test data are similar in the sense that the output became very erratic at temperatures above six or seven hundred degrees F. The test beams were pre-metalized Advac, Lucalox, and Duramic M120FT. It is felt that the bonding agent was responsible for the poor performance rather than the substrate material itself.

The other three types of ceramics tested were Aluminum Oxide, Cordierite, and steatite tubes with the gages embedded along the center line of the hole. In order to evaluate the thermal coefficient match, the bonded gage resistances were measured at each temperature and compared with the free filament gage resistance. The difference in gage resistance represents the amount of thermally induced strain on the gages due to the bond to the substrate material.

The data shows that the thermally induced strain is surprisingly small and that the thermal expansion coefficients of the ceramics are close to that of silicon. The main difficulty in the use of these ceramics as substrate materials lies in the fabrication and assembly with other materials. Some investigation, and design, of the ceramic element transducers was underway, but was discontinued in view of the favorable results obtained with the tungsten alloys.

c. Oxidized silicon substrate: The beam material selected was 5.5 ohm-centimeter n-type silicon with a thermally-grown oxide layer for isolation. The gage resistance changed only 1% after bonding to the silicon beam. A 4-ohm initial unbalance of the half bridge was observed and corrected by adding a decade resistance box to the low gage. The results up to 755°F showed a high apparent strain which is large because the additional balancing resistance is constant with increasing temperature. The test was stopped because of breakdown of the isolation to the substrate at around 700°F. It is felt that components (such as residual flux) in the brazing compound penetrated through the oxide layer. Here again, the use of silicon as a substrate material creates difficulty in fabrication and assembly.

d. Pure tungsten: Fig. 9 shows that tungsten has a thermal expansion coefficient closer to that of silicon than do other metals. Several specimens of tungsten substrate were successfully gaged and tested. One tungsten bar broke at a low stress level (13,500 psi) and it is felt that the tungsten was in an unwrought condition and had an unsatisfactory gain structure.

Gage resistance and isolation were measured over the range of 80°F to 700°F. The results are tabulated in Table 5.

Although the leakage resistance decreased substantially at 700°F, it was still about 4×10^5 times higher than the gage resistance and should contribute negligible error. The peculiar variation of resistance versus temperature may be due to the fact that the coefficients of expansion of silicon and tungsten (and, in fact, most materials) is non-linear over such a wide temperature range and these coefficients do not track each other.

e. Tungsten alloys: Two types of special tungsten alloys have been made for this contract. They are Alloys #955 and #982. The distinct advantages of these alloys over the pure tungsten are:

(1) while retaining low thermal expansion coefficients, they have relatively high yield strength (100,000 psi,) and

(2) they can be fabricated into transducer elements and components with conventional machining practices.

Bonded gage resistance measurements at various temperatures have been made, and the results on Table 6 indicate that Alloy #982 has a

thermal coefficient closer to that of silicon. However, there was no gage breakage when bonded to either alloy. Tests were continued on Alloy #955 in conjunction with Alloy #982 because of its slightly superior elastic properties.

All pressure transducers were constructed with either one of these two alloys. Some very promising results have been obtained and will be discussed in a later section. Because of the comparatively long delivery requirement in the manufacture of these alloys, few force loading experiments were performed. Instead, the alloys were tested with pressure as transducer diaphragms.

SECTION V

STRAIN TRANSMISSION EXPERIMENTS

Experiments have been performed on four different techniques of bonding semiconductor gages to various substrate materials. Data have been obtained for evaluation of these techniques in regard to the transmission of strain to the gages.

1. BONDING AGENTS

a. Ceramic cement: Cements from two manufacturers have been evaluated. Although the colors are different, the test results showed almost identical performances from both cements. They are Allen Type PBX ceramic cement and Trans-Sonics ceramic cements. The following gage application procedure was followed:

i. Roughen beam with 80 grit aluminum oxide paper.

ii. Clean in MEK and alcohol.

iii. Apply a precoat of cement per instructions and allow to dry.

iv. Wet precoat with fresh cement and wipe.

v. Put a puddle of cement in the middle of the bar and put the gage down into it.

vi. Cure: 1/2 hour at room temperature
2 hours at 200°F
1 hour at 400°F
1 hour at 600°F

Strain transmission data showed both cements are excellent in bonding the gages to the substrate.

We have encountered some difficulties when this cement was used on gages with silver leads. After exposure to high temperature, some components of these cements started to attack the lead wire resulting in an open circuit. After, consulting with the manufacturer, the leads were replaced with pure platinum wires, and there were no signs of any chemical attack.

The only drawback of these cements is that they are designed for use in very thin layers. Some gage application techniques required the cement to fill a void (embed gages in ceramic tubings). The cement can be applied by building up layers of fully-cured cement a small amount each time. This procedure was quite time consuming.

b. Pyroceram Brand Cement #45: The cement was designed by Corning Glass Works for sealing operations. The uncured cement, after complete evaporation of the vehicle (amyl-acetate) is chalky and does not

render a satisfactory seal. However, when the glass is fired directly, according to the prescribed schedules, a change in material occurs. The glass develops first a vitreous glass then, on further firing, a partially crystalline structure which results in a devitrified glass seal which is much stronger and harder than the original glass.

The selection of this glass for bonding the gages on the tungsten alloy 982 and 955 is based on the following properties of the glass.

i. It was designed for continuous service at 650°C.

ii. It has a coefficient of thermal expansion very close to that of the gage crystal. (See Fig. 9)

iii. It is chemically inert with pressure transducer components.

The curing cycle for this type of cement is farily elaborate, especially the tungsten alloy which oxidizes rapidly at the final cure temperature if fired in air. The following procedure was followed for the gage application.

i. Roughen diaphragm with #80 grit aluminum oxide paper.

ii. Clean in MEK and alcohol.

iii. Apply a precoat of Pyroceram.

iv. Oven dry at 240°F for 20 minutes.

v. Apply a puddle of fresh Pyroceram in the proper locations.

vi. Apply gages in the fresh Pyroceram.

vii. Oven dry at 240°F for 20 minutes.

viii. Examine and check for proper gage location.

ix. Preglaze at 1200°F in air for 1 hour. Heating rate is kept at approximately 25°F per minute.

x. Cool to room temperature at a rate of 8°F per minute.

xi. Place the diaphragm in a specially designed stainless steel container and flush the interior with forming gas continuously.

xii. Increase the temperature to 1400°F for 1 hour and cool to room temperature.

The heating and cooling rates are kept at 6°-10°F per minute. When cured, the appearance of the glass is very similar to the ordinary household Corning Ware.

c. Brazing of gages: This method was developed for attaching silicon gages to metallized ceramics and oxidized silicon load carrying substrate. Satisfactory results have been obtained with Hanovia Silver Paste #521 which is a viscous suspension of finely divided precipitated or flaked silver in an organic vehicle. Other metallizing and brazing materials tested were Hanovia Liquid Silver #228, Eutec-Silweld 1618, Silvaloy #45, Silvaloy #60, and Easy-Flow #6040. The Liquid Silver is fundamentally the same as Silver Paste #521, and the others are high silver content brazing alloys. An optimum firing cycle was developed using a Hoskin's tube-type electric furnace.

While the data showed satisfactory results below 500°F, all gages bonded with this method became noisy and unstable at higher temperatures. It is quite likely that the ohmic contact is subjected to excessive stress due to the different thermal expansions of the materials involved. Separation between the silver brazing compound and the contact leads was also observed. Further evaluation of this technique was discontinued.

d. Flame Sprayed Gages: The services of the RdF Corporation of Hudson, New Hampshire, were employed to apply semiconductor strain gages to various materials using plasma jet and Rokide processes.

Four pieces of 17-4PH stainless steel 1/8 x 1/4 x 1-1/2" were sand blasted and coatings of aluminum oxide .7, 1, 2, 3, mils respectively were applied. These specimens plus one tungsten beam, also coated, were prepared for metallizing at a later date.

The Lucalox ceramic beam was prepared and a .002" plasma coat applied. The application was not satisfactory. The coat would not adhere to the ceramic and could be removed with the thumb nail.

Two tungsten beams were then prepared and coated on both surfaces with .002" plasma. The leakage to ground at this point was 3K megohms with 50 volts applied.

The P silicon gages with silver bonded leads were held in place over the precoat with Teflon tape. Small pieces of tape were placed over the lead area on both ends and a small strip across the center.

Varied methods of application were used with the plasma but in all cases the filaments were destroyed.

The steps followed were:

i. Normal application which consists of holding the gun approximately 8-12 inches from the work and passing the flame across the work from side to side.

ii. Bringing the spray across the gage at 90° to the surface to

help eliminate possible lift of the gage due to back pressure from the surface.

iii. Applying the plasma from a distance and working straight in on the piece.

From the investigation of these 3 steps, it was concluded that the concentration and the velocity of the particles caused the filaments to break.

The tungsten pieces were reblasted and a .002" precoat of plasma applied. The gage was held as previously mentioned and an overcoat of Rokide applied. This combination proved more successful in that the gage was still intact after the Rokide application. However, there was no electrical continuity so the tape was carefully removed and it was found that the gage had broken where the tape held the filament.

A second attempt was made and this time the gage was unbroken. The tape was then very carefully removed so a coating to fill in the tape voids could be made.

Watching the tape removal through a microscope, it was noted that as the tape peeled the filament twisted and snapped. The tape held to the gage surface too tightly. The investigation was stopped at this point.

In concluding, this type of application for semiconductor gages by the flame spray method is possible. The technique of application will have to be established in order to reduce the large amount of breakage which is evident at this time. No further work was performed in this area.

2. TEST EQUIPMENT FOR STRAIN TRANSMISSION

A Blue M type E-514A muffle furnace with electronic temperature control over the temperature range of 100°F to 1800°F was purchased and adapted for running strain transmission tests on beam-type elements at elevated temperatures. It was elected to begin tests on beam-type elements at elevated temperatures. It was elected to begin tests on beam-type elements rather than columns or pressure transducers since this configuration can be tested most readily. Later the oven was further modified for tests on breadboard pressure transducers.

A sketch of the beam testing setup in the oven is shown in Fig. 10.

3. TEST RESULTS

The following strain transmission experiments include beams made of tungsten, Ni-Span C, Silicon, and three types of metallized ceramics. There were no data on force loading of the tungsten alloys finally chosen for the

construction of pressure transducers. This omission was necessitated by the long delivery requirement of these tungsten alloys. Instead, test data on the pressure transducer testing clearly indicate that strain transmission has been successfully achieved.

a. Tungsten Beams: The tungsten beam was hydroblasted at the RdF Corporation, Hudson, New Hampshire. A precoat of the PBX was applied and two silicon gages with .01 ohm-cm were placed on the beam before curing with the temperature cycle as reported under Bonding Agents. As in the previous case, the gage resistance increased several ohms indicating that the gages were preloaded in tension due to the lower coefficient of thermal expansion of tungsten.

Fig. 11 summarizes the apparent strain and the change of sensitivity at various temperatures up to 995°F. One pound dead weights were used to obtain the maximum non-linearity (the deviation of the output change at different loading levels from the theoretical straight line). The non-linearity, zero shift after each loading, and electrical leakage to ground (beam) are tabulated in Table 7.

The amount of zero shift (change of the no-load output) after each loading is in the order of one-tenth of one percent of the full scale output which, at room temperature, is approximately 480 microinches per inch. It is also noted that the maximum non-linearity is less than 1/2% of the full scale output at all temperature except 241°F. These facts indicate that the transmission of strain to the load carrying member is achieved with high efficiency.

The apparent strain, as shown on Fig. 11, changes more than 100% of the force output at room temperature. This change does not indicate that a hundred percent zero T.C. will be required for this assembly since the force output level is low in this experiment. As the force output level is increased, the percent of compensation is reduced proportionally.

It is also felt that the initial sharp rise before 500°F and the subsequent drooping between 500°F and 700°F could be caused by distortion of the gages. Any improvement in the bonding technique should reduce this large variation to within the compensatable range.

The sensitivity decrease with temperature, as shown on the same figure, is approximately 48% as the temperature increases from 72°F to 995°F, or .05% per °F. Fortunately the change is very linear as compared to the apparent strain. Consequently, the span temperature compensation represents an easier task.

b. NiSpan C Beams: Two beams made of NiSpan C were hydroblasted at RdF, Hudson, New Hampshire. One was precoated with PBX cement and the other with Englehard CA9R cement which was recommended by RdF. Two silicon gages were bonded to each of the beams with respective cements. The bonded gage resistance decreased slightly indicating an initial compression of the gages when bonded with Englehard CA9R cement.

During load tests, this beam showed excessive creep and zero shift with each loading. This beam was not considered for further testing.

The beam with PBX cement was tested at temperatures up to 600°F. The reduced data is tabulated in Table 8.

Since the gage factor is approximately 115, the strain level from loading is 370 microinches per inch.

It was also observed that both the non-linearity and the zero shift after each loading was less than .2% of full scale force output which indicates that the strain transmission was achieved as efficiently as in the case of the tungsten beam bonded with PBX cement.

A study of the gage resistances at various stages of this bonding technique revealed some interesting facts. The resistance values are shown on Table 9.

The above data indicates that not only the difference in thermal expansion coefficients determines the prestrain on the gages, but the cement and the bonding techniques also affect it to a large extent. Also note that the fracture of the gages occurred around 600°F. At this temperature, the thermally induced strain is expected to be at most 1000 microinches per inch. The gages have been known to be able to withstand much higher strain levels, and consequently it is speculated that the fracture is caused by one or a combination of the following:

i. During the curing of the cement, distortion is set in (such as buckling or twisting) resulting in a very highly stressed area in some portions of the gage.

ii. Non-uniformity in the cross section of the gage along the unbonded strain sensitive portion could cause a very localized elongation.

iii. The existence of micro-cracks in the gage and subsequent propagation when stressed in tension could result in a fracture. The noisiness and discontinuities of the output observed before fracture could be caused by this fact.

iv. Strain on the substrate is transmitted to the gage by the ohmic contact areas only. The highly stressed junction could easily fail under this condition, and it also can be the source of the noise at high temperatures.

c. Silicon Beam: One silicon beam was gaged by brazing with #521 Silver Brazing Compound. The gage resistance changed only slightly after bonding. The following result shows that the strain transmission of approximately 370 microinches per inch was satisfactory, but the thermal span sensitivity coefficient is surprisingly high. The shunting effect of the low leakage resistance is partly responsible for the low output at high temperatures.

Test was stopped due to low leakage and erratic output at 755°F as shown by the data on Table 10.

The low leakage at 755°F is probably caused by the penetration of the brazing compound into the pre-grown oxide layer.

d. Ceramic Beams: Three different types of premetalized ceramic beams have been tested. They are Advac, Lucalox, and Duramic M120FT. The test results shown on Table 11 are similar in the sense that the transmission of 120 microinches per inch from the Lucalox and Advac beams and 530 microinches per inch from the Duramic beam was satisfactory. As the temperature increases over 500°F or 600°F the output became very noisy and erratic.

From the results of these tests, it is felt that the stresses induced by differehce of thermal expansions is in excess of the yield strength of the silver brazing compund (#521) at temperature above 500°F.

SECTION VI

TRANSDUCER DESIGN

Three different types of pressure transducers were considered. The first two types consisted of a pressure summing diaphragm which generated a force to the element. An electrical signal results when the strain on the element is transmitted to the strain gage. The third type of construction employs the tensile and compressive stresses on a gaged diaphragm to obtain the electrical signal directly without the use of a force measuring element. The advantages and disadvantages of each design will be discussed briefly. Due to the time limitation, only the gaged diaphragm design was actually constructed and tested.

1. DIAPHRAGM WITH SHEAR BEAM ELEMENT

The design of this construction has been proven successfully through our previous experience. Modifications must be made to accommodate the high temperature application. The design, as shown schematically on Fig. 12, consists of a pressure port together with a metallic "O" ring to contain the pressure medium. A gaged shear beam is attached to the center of the diaphragm. When an external pressure is applied, the electrical signal from the gages measures the force generated by the differential pressure across the diaphragm. An evacuated and sealed reference chamber is created by heliarc welding a housing to the rigid rim of the diaphragm so that variation in temperature and atmospheric pressure do not affect the output of the transducer. At the same time, the gages and compensating network are protected from any corrosive and oxidizing environment to which the transducer may be subjected. The electrical signal is brought out by means of a high temperature connector or header.

The shear beam element employed in this design is proprietary to Schaevitz-Bytrex. Two gages perpendicular to each other are placed on the opposite surfaces of the sensing section along the direction of maximum shear strain. The holes serve the purpose of maximizing the strain on the gages and locating the gages during bonding. The flexure on the other side of the center line guides the deflection of the stem and diaphragm along the axis perpendicular to the diaphragm so that no eccentric distortion results when a pressure is applied.

The advantages of the design are:

a. The strain gages are located very close to each other so that it will be relatively insensitive to transient thermal effects.

b. The strain sensitive section is on a force measuring element. If the diaphragm is subjected to a thermal shock, the heat is conducted to the element through balanced heat sinks so that the effect of the shock is greatly reduced.

c. Due to the small deflection of the shear beam, the transducer will have a high natural frequency.

d. The transducer is relatively simple since there are only two parts (diaphragm and element) in the pressure measuring assembly.

On the other hand, the disadvantages are:

a. Brazing of the element to the diaphragm must be controlled carefully so that no misalignment results.

b. The brazed joint could be weakened by thermally induced stresses.

c. Variation in gage resistance after bonding to the element could cause excessive nonlinear apparent strain with temperature variation.

2. EMBEDDED GAGE CONSTRUCTION

This design is similar to the previous one in the sense that a pressure summing diaphragm is employed to generate a force to the element. The element is made with small diameter tubing with strain gage embedded along the center line. Fig. 13 shows an assembled pressure transducer.

The main advantage of this design is that cured gaged columns can be selected separately before assembly. If the resistances were closely matched, and assuming there is no change during gold brazing, the apparent strain due to temperature can be minimized. It is offset, however, by a relatively complex assembly and brazing procedure as compared to the previous type of design. Other than these factors, the characteristics are similar to the shear beam type transducer.

3. GAGED DIAPHRAGM TRANSDUCERS

The design of this transducer is based mainly on the experimental results of several models gaged with conventional type strain gages. Fig. 14 shows an assembly of this type of transducer. When a diaphragm is subjected to an applied pressure, both tensile and compressive stresses are distributed on the surface. Gages are placed along the radius to measure these stresses which, of course, is proportional to the applied pressure. The taper on the diaphragm's cross section provides a more uniform stress distribution as well as extends the range of linear bending stresses which the gage measures.

The gaged diaphragm transducer has three distinct advantages over the others.

a. It measures the pressure directly without any intermediate structural members. Its simplicity results in the elimination of common sources of error and undesirable characteristics in other types of pressure transducers.

b. Transducer machining and assembly is simple.

c. Due to the small mass of the sensing element (diaphragm) it has a very high natural frequency.

The main disadvantage of the design is that the gage section is directly in contact with the pressure medium. Consequently a thermal diffuser on the pressure adapter is required to protect diaphragm from thermal shocks. A typical design is also included in Fig. 14.

Since the gages are bonded directly on the diaphragm, the diaphragm material selection is limited to low thermal expansion alloys. Since the diaphragm is directly exposed to the pressure medium, the corrosive resistance at high temperature must be investigated.

All the prototype transducers employed this type of design, mainly because of the simplicity in construction. Both types of tungsten alloys were used. Later experiments have shown that although some oxidation of the material was observed, nickel plating on the tungsten alloys showed a marked improvement.

SECTION VII

PRESSURE TRANSDUCER EVALUATION

1. TEST EQUIPMENT

Figure 15 shows the arrangement of the apparatus used in the high temperature measurement experiment. A conventional pressure transducer of a proven design was made to be used as a pressure standard. This standard transducer was calibrated with an oil dead weight primary pressure standard which is traceable to the National Bureau of Standards. Table 12 shows the actual output characteristics of the pressure transducer. A bottle of dry nitrogen together with a pressure regulator was used to generate the desired pressure levels using data on Table 12 to both the standard pressure transducer and the test specimen.

2. TEST RESULTS

a. First prototype transducer: A pressure transducer was constructed using tungsten alloy #910 previously tested for compatibility with the silicon gages. The design was similar to the gaged diaphragm type construction reported in the last section with some minor modifications because of the size of the material available at that time. The diameter of the stock was 1-1/4 inches instead of 2 inches, and consequently the use of metallic "O" ring and bolted-on pressure adaptor was impractical. The pressure port was silver soldered onto the pressure senitive diaphrag. Fig. 16 shows the assembly of the transducer tested.

The gages were bonded to the diaphragm with Trans-Sonic High Temperature Cement. The diaphragm surface had been sandblasted before a thin precoat was applied. The gages were bonded and cured with the temperature cycle reported previously. Due to the unpredictability of the bonded gage resistance, several pairs of gages were applied at the same time so that a pair of closely matched gages could be used for actual pressure loading and temperature compensation.

After the selection of a pair of gages, ceramic insulated wires were attached to the silver leads on the gages. Two relatively high valued fixed resistors were employed to complete the bridge outside of the high temperature region.

Table 13 shows the actual data obtained on the gaged diaphragm transducer. After gage failure at 430°F, the diaphragm was regaged and tested up to 787°F.

In the vicinity of 1000°F, the gage leads broke again. Close examination revealed that the ceramic cement attacked the silver leads slowly at higher temperature. This attack is accelerated in the region where the interface is exposed to air. It was rather unfortunate to discover this chemical reaction at this late stage of the project--the main reason being that on previous evaluations the duration of exposure to elevated temperatures was only two or three hours; whereas, in this experiment the transducer was subject to high temperature over 20 hours before failure occurred.

However, the above data showed some very encouraging results. The output signal characteristics will be discussed separately below:

i. Data up to approximately 800°F indicate that the use of tungsten alloy is feasible for high-temperature pressure transducer elements. At full scale pressure the strain level is over 700 microinches per inch, and yet the creep from the material is less than 1/4% after the initial loading at temperature.

ii. The non-linearity, defined as the deviation from the straight line output between zero and full scale pressure, is less than .3% up to 300°F. It increases up to 1.46% before dropping back to .3% at 787°F. Temperature effects as discussed below could be responsible for this variation.

iii. The data showed that the hysteresis is almost 2% at higher temperatures. It is defined as the maximum difference between the output with increasing and decreasing pressure at the same pressure level. It is felt that this excessive hysteresis could be caused partly by the cooling effect of the entering pr ssure medium at room temperature as well as the adiabatic cooling wh n the pressure is released. Also, the silver soldered pressure port is not .s rigid an assembly as one would expect from best transducer structure with respect to hysteresis. This problem will be eliminated on future transducers which have a bolted-on pressure port.

iv. The zero shift, defined as the difference between no-load output before and after a particular pressure loading, is in the order of 1/2% of the full scale output. The cooling effects mentioned previously could be partly responsible for this shift since the temperature of the pressure sensitive diaphragm is different before and after the pressurization. The data in Tables 2 and 3 represent the results obtained after exercising the transducer to full scale pressure before the actual run. During the initial run at each temperature (first exercise) the zero shift is somewhat higher.

v. Unfortunately no reliable data on the apparent strain have been obtained for the transducer due to the zero shift at each temperature. It had been planned to obtain this information at various temperatures without pressure loading before the gage lead failure. It is reasonable to assume that by selecting closely matched gage resistances after bonding the compensation is a simple task.

vi. The full scale output in millivolts per volt decreases with increasing temperature. Fig. 17 shows the variation is fairly linear with a coefficient of approximately .04% full scale per °F. Since the gage resistance increases rather linearly with temperature, the originally proposed technique of self compensation with series resistance could be employed.

This transducer was discontinued from testing because of the impracticality of further gage replacement.

b. Second group of prototypes: The first prototype transducer was made from a sample material. Two inch diameter stock was ordered, but shipment could not be made within one month. During this waiting period, a similar tungsten alloy (Alloy #955K) was used to make several pressure sensitive diaphragms and pressure ports (see Fig. 14). Test data showed that this new alloy was inferior for transducer application in the sense that it oxidized more severly and exhibited excessive creep when stressed at higher temperature.

The gages were bonded to the diaphragm by Pyroceram type cement #45 because of the chemical attack on the silver lead wires by ceramic cement. Measurement of gage resistances after bonding indicates that the gages are in compression since the tungsten alloy substrate has a slightly higher thermal expansion coefficient. The actual resistance change in all the gages applied is very uniform as compared to those bonded with ceramic cement. This fact is encouraging because the task of compensating for apparent output with temperature is greatly simplified if the bonded gage resistance is matched very closely. The close matching of the resistance can be achieved by selecting equal resistance unbonded gages since the change of resistance is uniform during bonding.

The first sample was fired in air up to 1400°F. The oxidation was so severe that the cement together with the gages, although fully cured, was lifted from the substrate. Two steps were taken to combat the oxidation. One was to fire the cement in forming gas as previously discussed, and secondly, a nickel plating was applied to the tungsten alloy. The nickel plating was successful and adhered well to the substrate at room temperature although some blistering occurred at temperatures above 1000°F. An attempt was made to bond the gages on the nickel-plated surface with Pyroceram without much success due to poor adhesion. The gaging area, consequently, has been masked during the nickel-plating operation. The Pyroceram, after firing, provides a hermetic seal against oxidation on the unplated areas.

One sample was prepared with the above modifications in gage application. The test history of this unit is shown on Tables 14 through 17.

After testing the sample at room temperature (Table 14), the transducer was heated to 227°F. After a full scale pressure was applied, the output continued to creep upwards for almost 5 mv/v before it became stable enough to be tested for linearity. During the second loading the total creep was decreased to approximately 0.2 mv/v. The data on Table 15 represent the results after loading to full scale three times.

During this shift or permanent deformation of the substrate material, the gages were also permanently strained. This residual strain is accumulated each time the permanent deformation takes place at various temperatures.

The sample was brought to 548°F. The unit continued to creep as indicated by the zero return on Table 16.

Table 17 shows the results at 235°F after the transducer was cooled from 548°F to room temperature and reheated to the test temperature. The data revealed two interesting features.

i. The non-linearity characteristics changed considerably from the data on Table 15 at 227°F. This change indicates that no-load neutral position of the sensing diaphragm has changed due to the accumulative permanent deformations.

ii. The amount of initial creep and zero shift was greatly reduced as compared to the data on Table 15. The increase in stability resulted from the fact that it had been loaded with full scale pressure at higher temperature (548°F). It appears that the yielding or permanent deformation occurs only once at particular temperature levels. The transducer was heated to 1200°F and a full scale pressure was applied. It was hoped that the transducer would be stabilized after this operation. However, the gage failed at around 500 psi. It is felt that the strain level was excessive due to the residual strain from previous deformations.

c. Third group of prototypes: Several transducer sensing diaphragms and pressure ports were machined using previously tested tungsten Alloy #982. Both Trans-Sonic ceramic cement and Pyroceram cement were used to gage the prototypes, but only one diaphragm gaged with Trans-Sonic cement was evaluated and partially temperature compensated over 1000°F.

Table 18 shows typical results of pressure loading data at various temperatures without any compensation. The transducer was energized with a regulated constant voltage source of 3 volts D.C. Fig. 18 shows the uncompensated span change and the apparent strain with increasing temperature. Due to the zero shift at each temperature, the apparent strain data were taken prior to any pressure loading.

Figure 18 shows the apparent strain is approximately 6% full scale through the entire temperature range. With any compensation, this figure could be reduced easily to 2% per approximately 900°F.

The main reason for the poor zero return is the relatively high strain level (700 microinches per inch). Due to the unexpected linear temperature coefficients, it is felt that transducers operating with lower strain levels would be more feasible.

The span changed from 37.54 mv/v at room temperature to 19.89 mv/v at 958°F or approximately 0.05% full scale per degree F. The "self-compensation" circuit, utilizing the increase in gage resistance with temperature) was placed in series with the transducer bridge, but the test result showed that this technique left the transducer slightly under compensated. Consequently, a constant regulated current source was used to power the transducer. This approach is equivalent to increasing the

constant series resistance infinitely so that the variation in bridge resistance does not affect the amount of current flowing through the gages. Since the gages were designed so that the percentage of resistance change per degree F is approximately equal the percentage of gage factor decrease, the increase in voltage drop across the gages due to resistance increase offsets the loss of gage factor.

The bridge completion resistors have also a secondary effect on the compensated output voltage since it affects the bridge resistance variation with temperature.

The bridge was initially completed with 10,000 ohm resistors. The span change from room temperature to 1015°F was approximately +5% for the entire temperature range. The completion resistance was consequently lowered to 2,500, 1,000, and 500 ohms and the span change was +4%, +3%, and -1% respectively. 600 ohm bridge completion resistance was finally selected. Room temperature output was 3.00 mv/ma, while the output at 1020°F remained essentially the same (within 0.05%). Although the transducer was perfectly compensated for the two end points, the output is slightly lower in variation with temperature (see Fig. 18). This error is approximately 6% full scale for 900°F. However, it can be reduced by compensating between 572°F and 1112°F as required by the Statement of Work for this contract. Fig. 18 shows that the variation of output due to temperature is perfectly linear beyond 500°F. Consequently, a zero temperature coefficient could be approached by carefully selecting the proper bridge completion resistance.

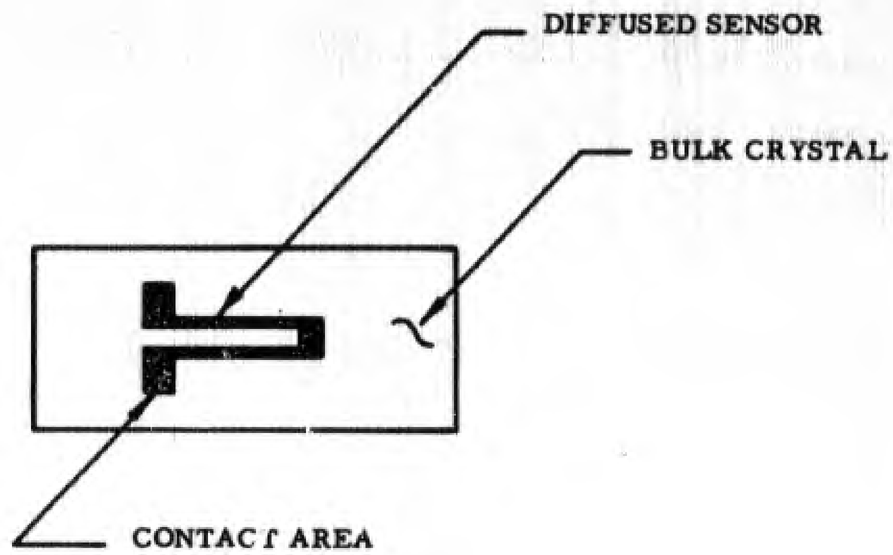

SENSOR DIMENSIONS

OVER-ALL LENGTH OF SENSOR	.070"
ACTIVE LENGTH	.050"
ACTIVE WIDTH	.001"
END CONTACT AREAS	.010" x .010"

DIFFUSED SENSOR
FIGURE 1

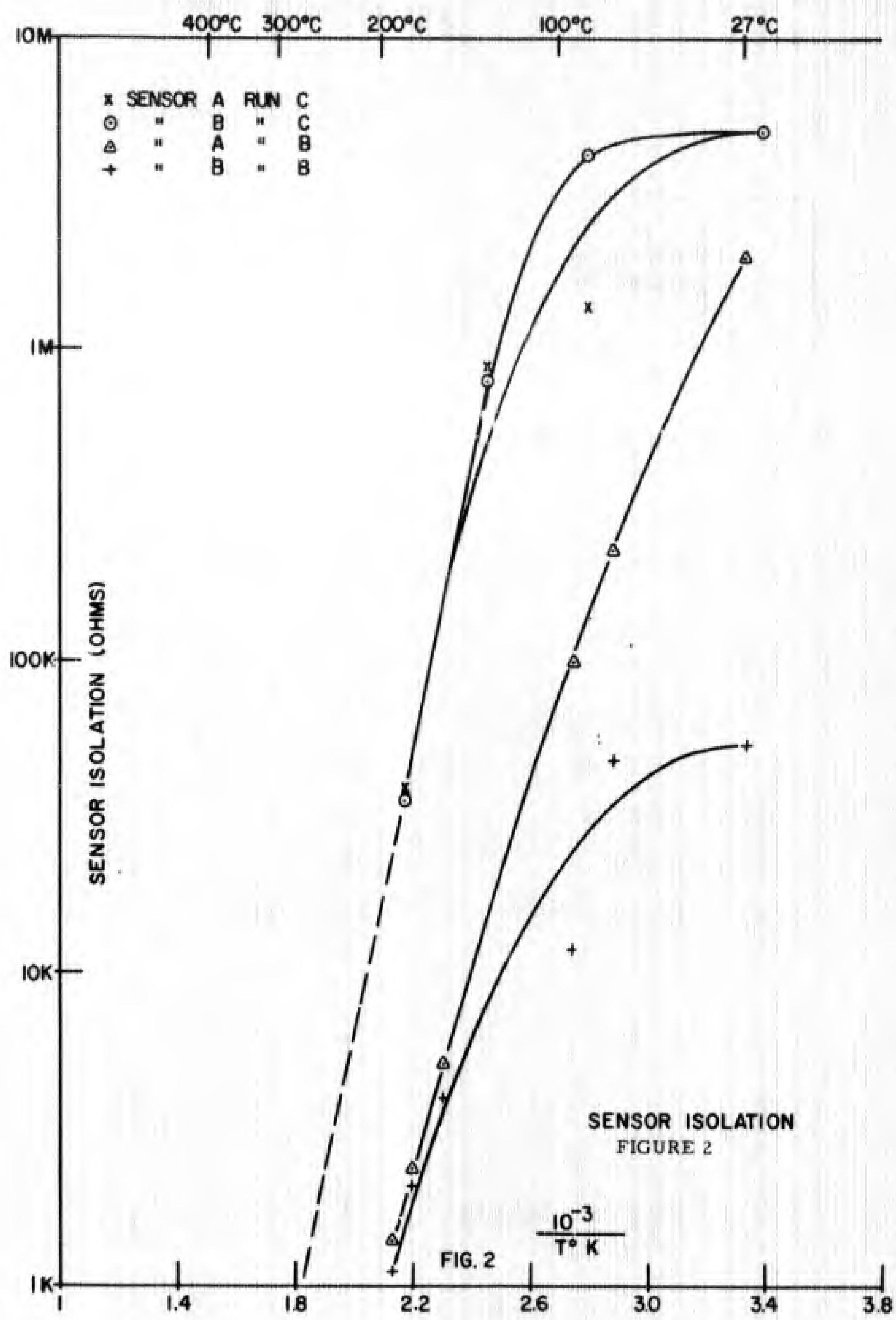

SENSOR ISOLATION
FIGURE 2

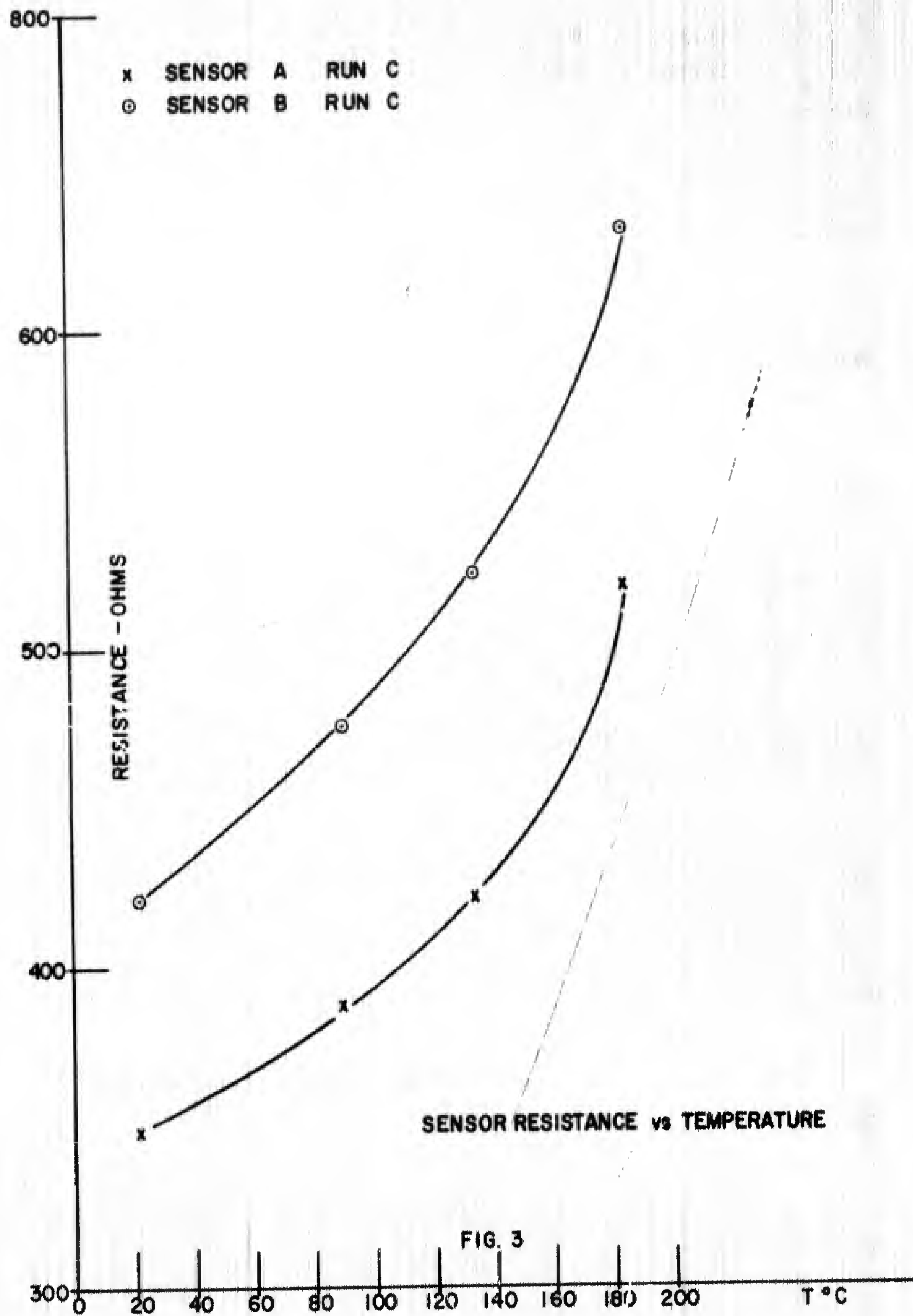

FIG. 3

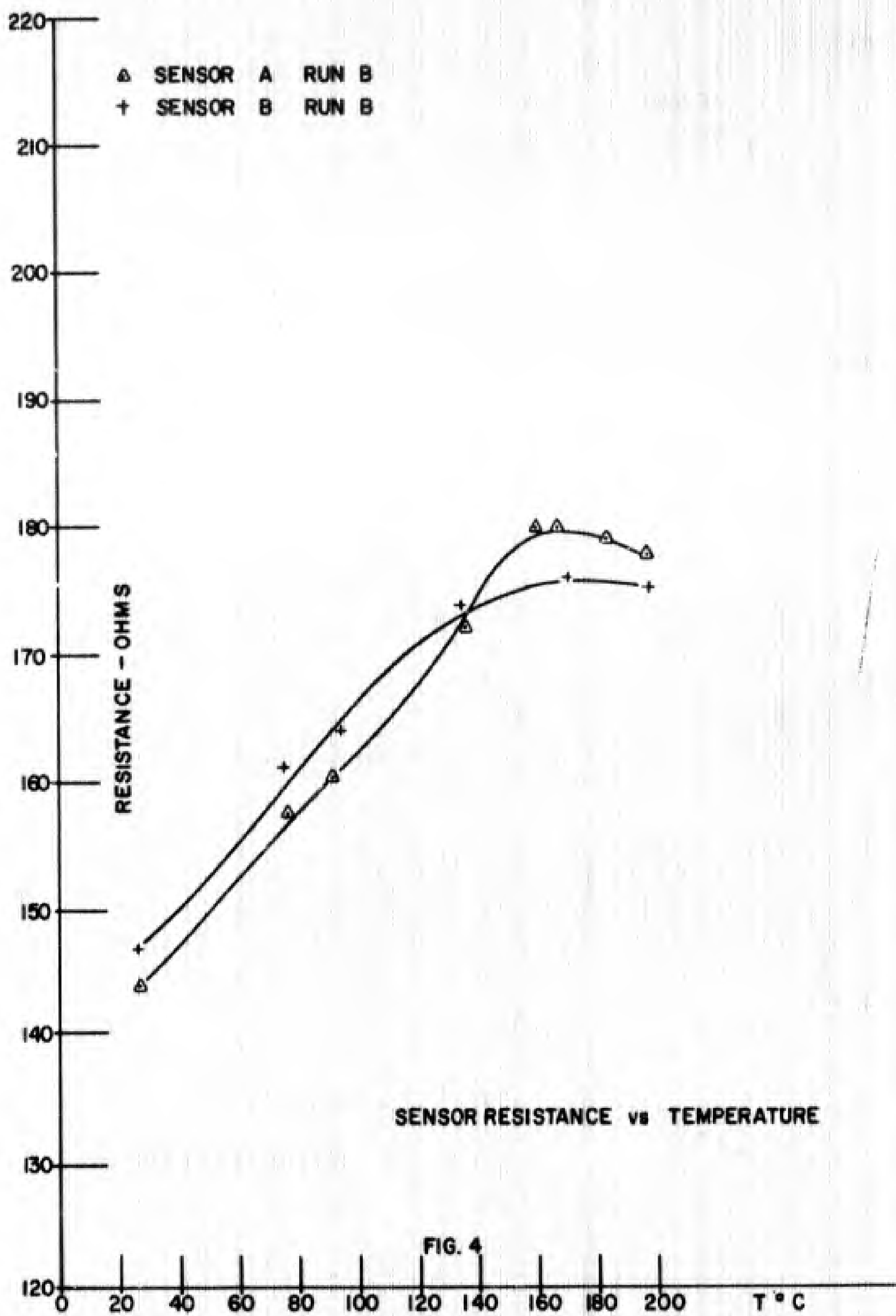

FIG. 4

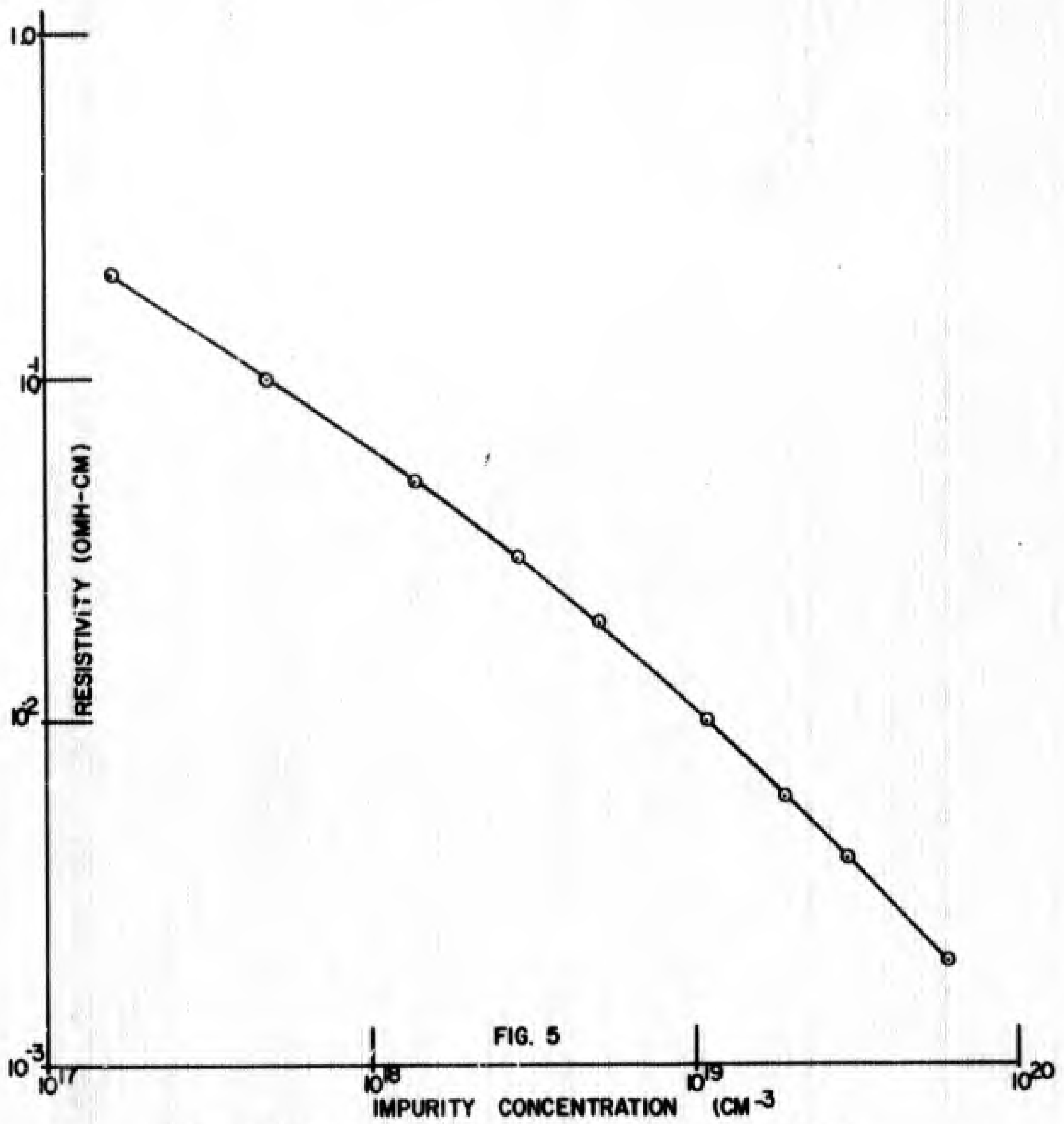

RESISTIVITY OF SILICON AT 300°K AS A FUNCTION OF ACCEPTOR CONCENTRATION. (P-TYPE)

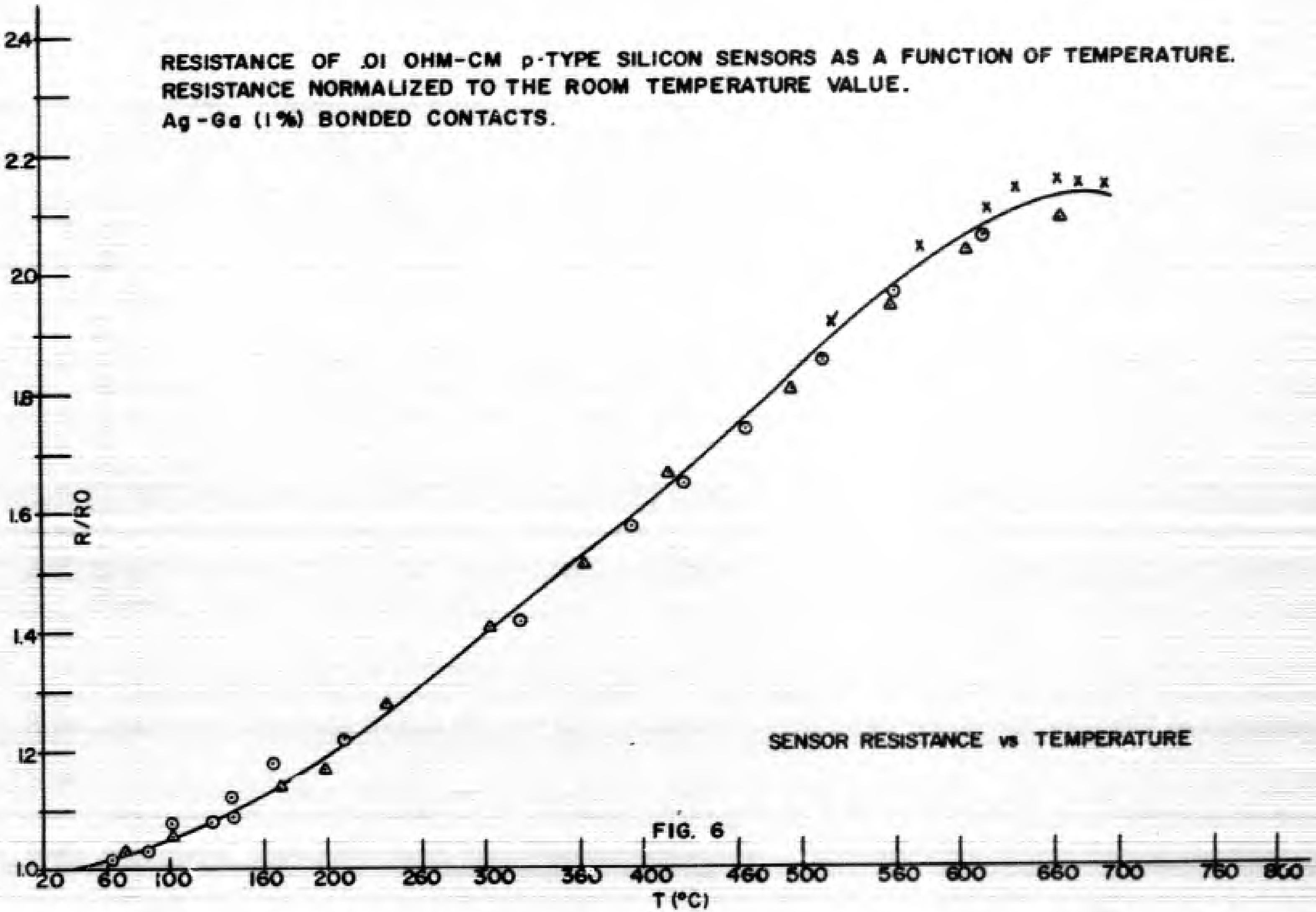

FIG. 6

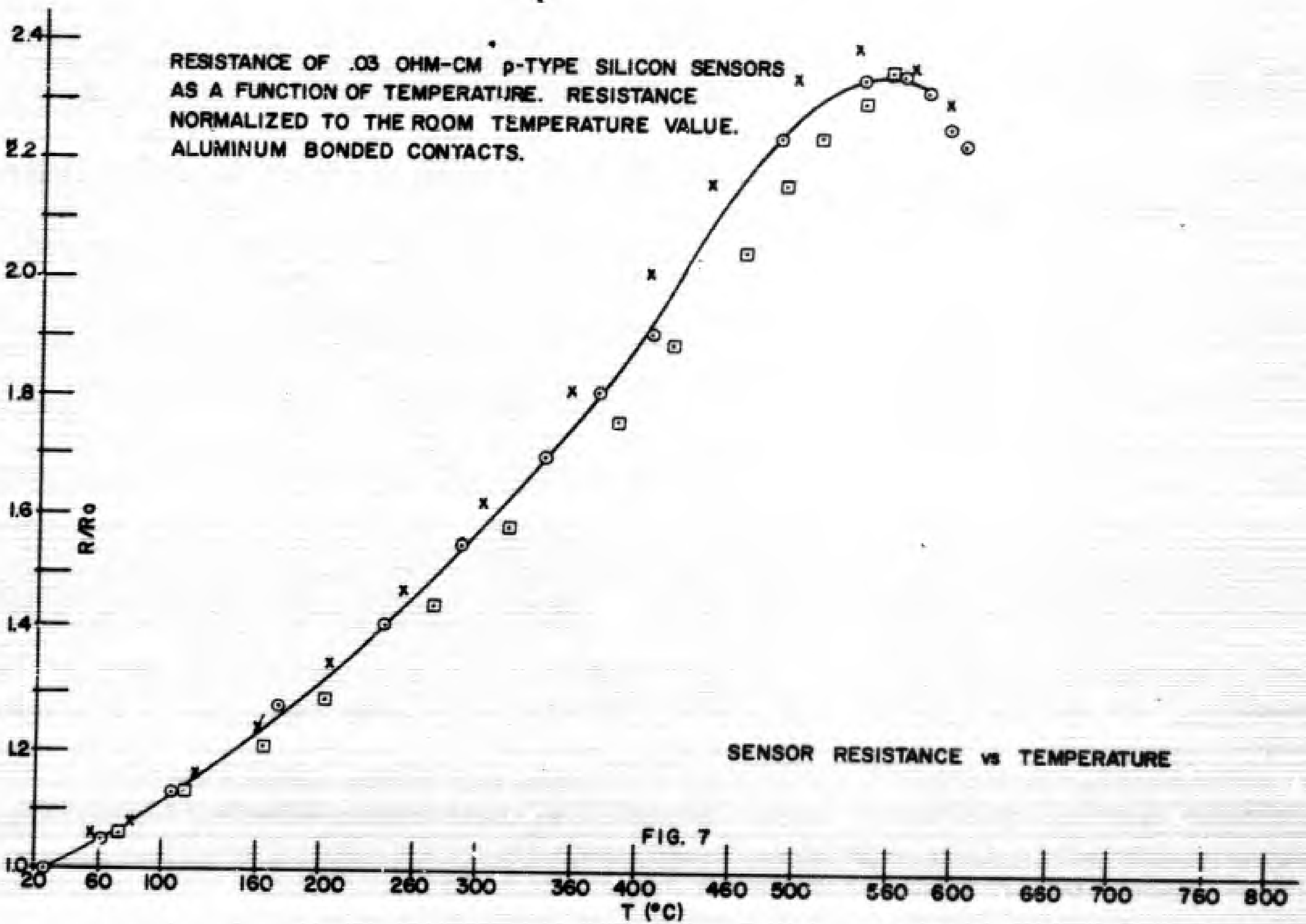

FIG. 7

SENSOR RESISTANCE vs TEMPERATURE

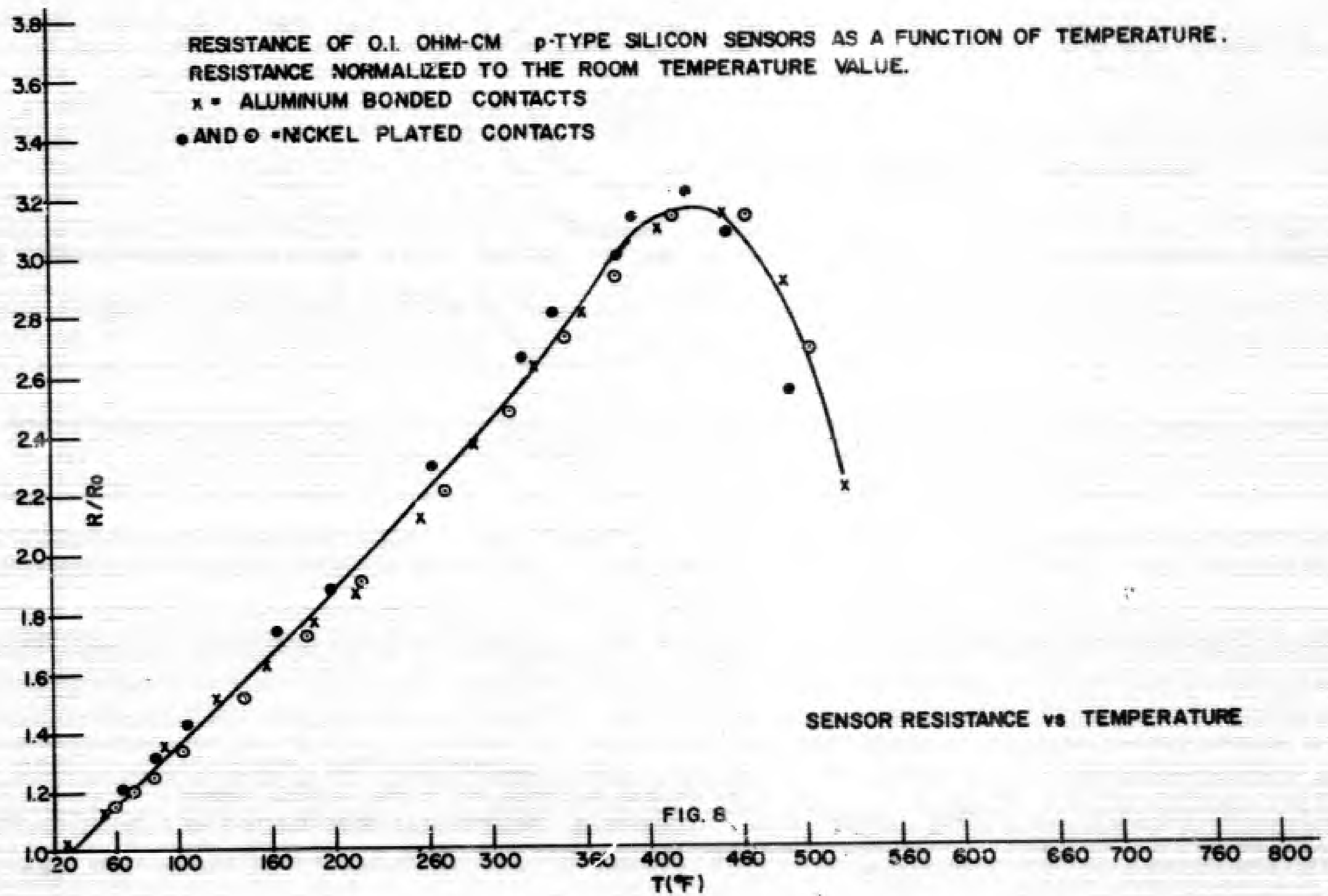

FIG. 8

SENSOR RESISTANCE vs TEMPERATURE

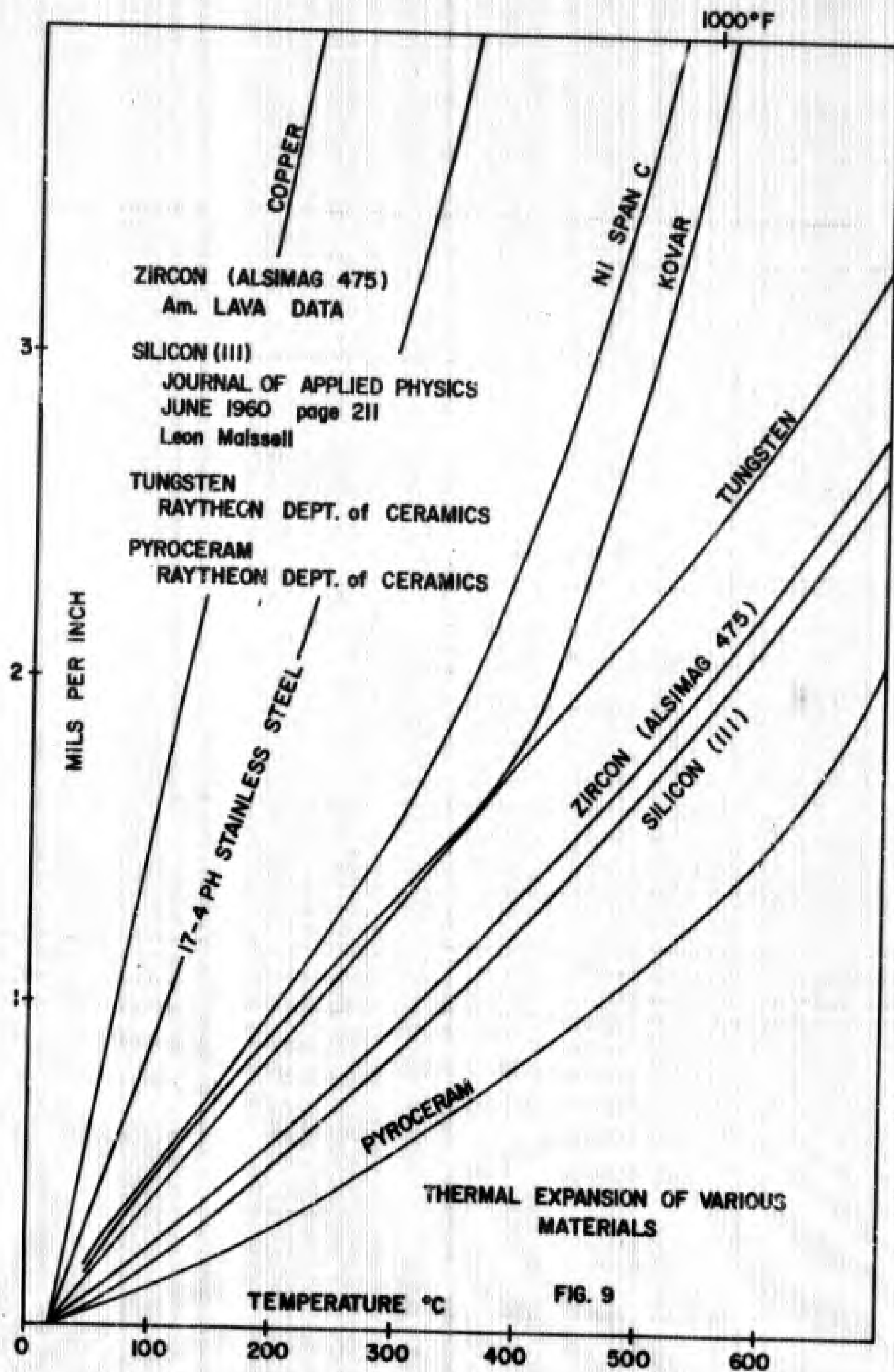

THERMAL EXPANSION OF VARIOUS MATERIALS

FIG. 9

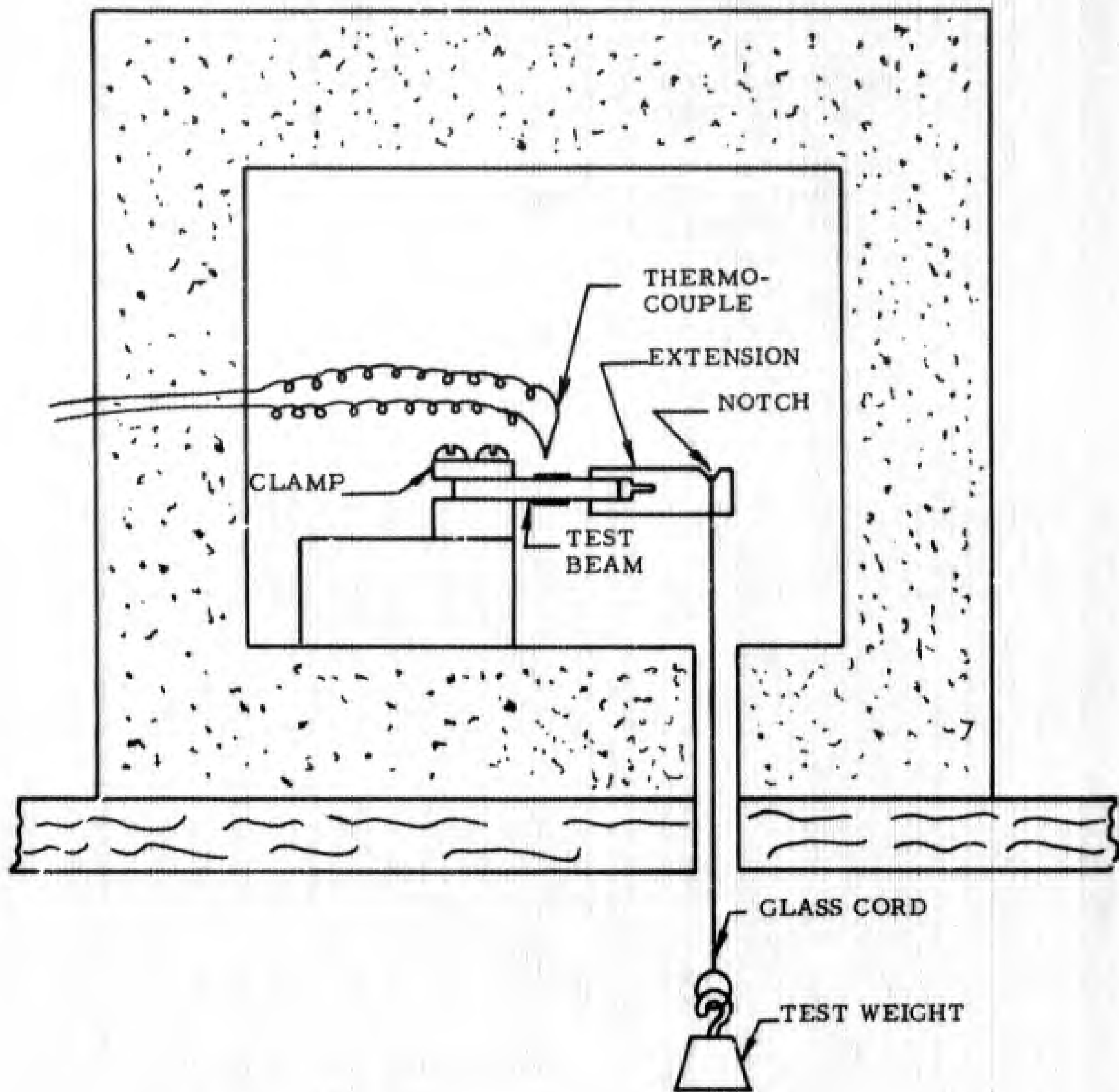

ELEVATED TEMPERATURE BEAM TEST SETUP

FIGURE 10

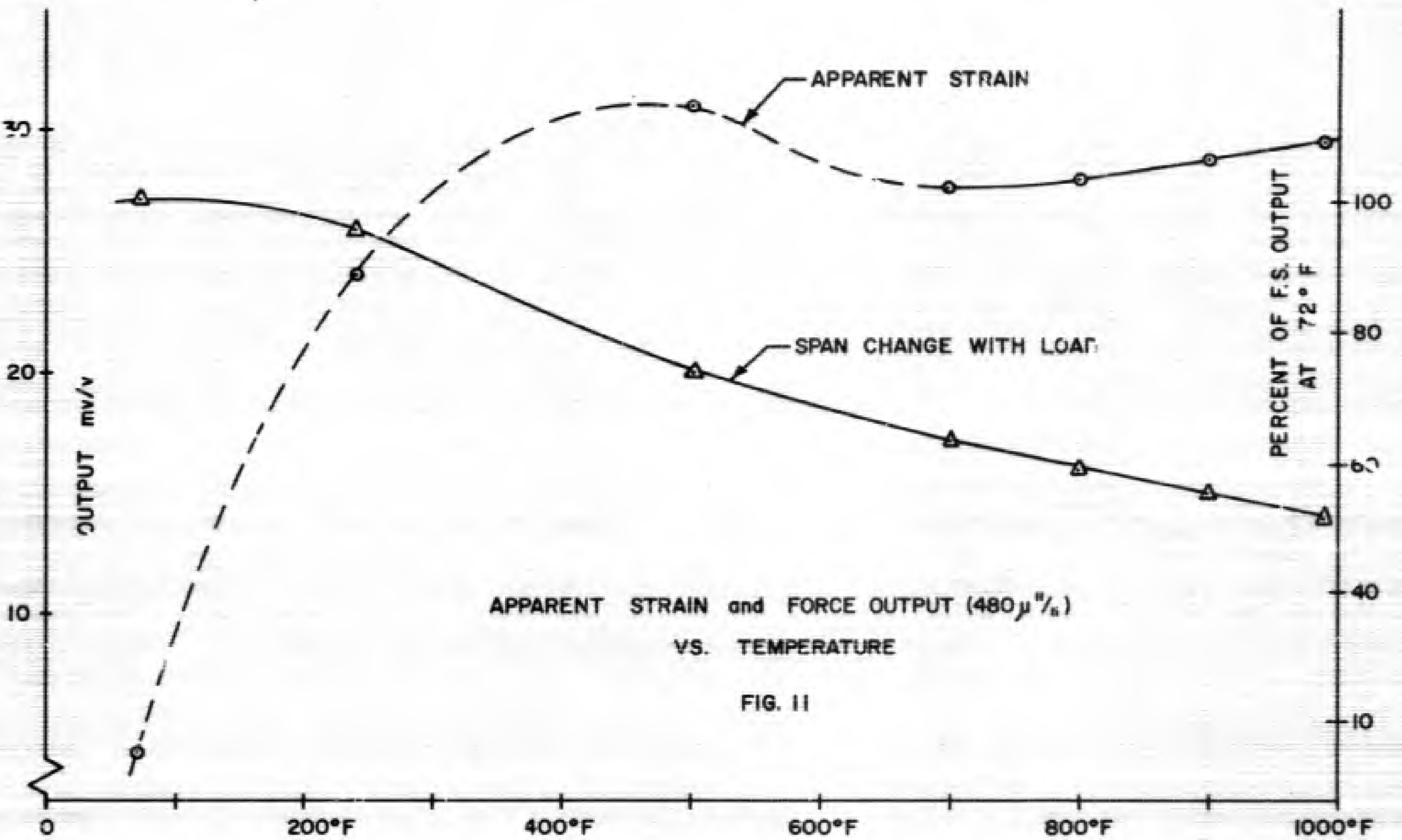

APPARENT STRAIN and FORCE OUTPUT (480μ"/") VS. TEMPERATURE

FIG. 11

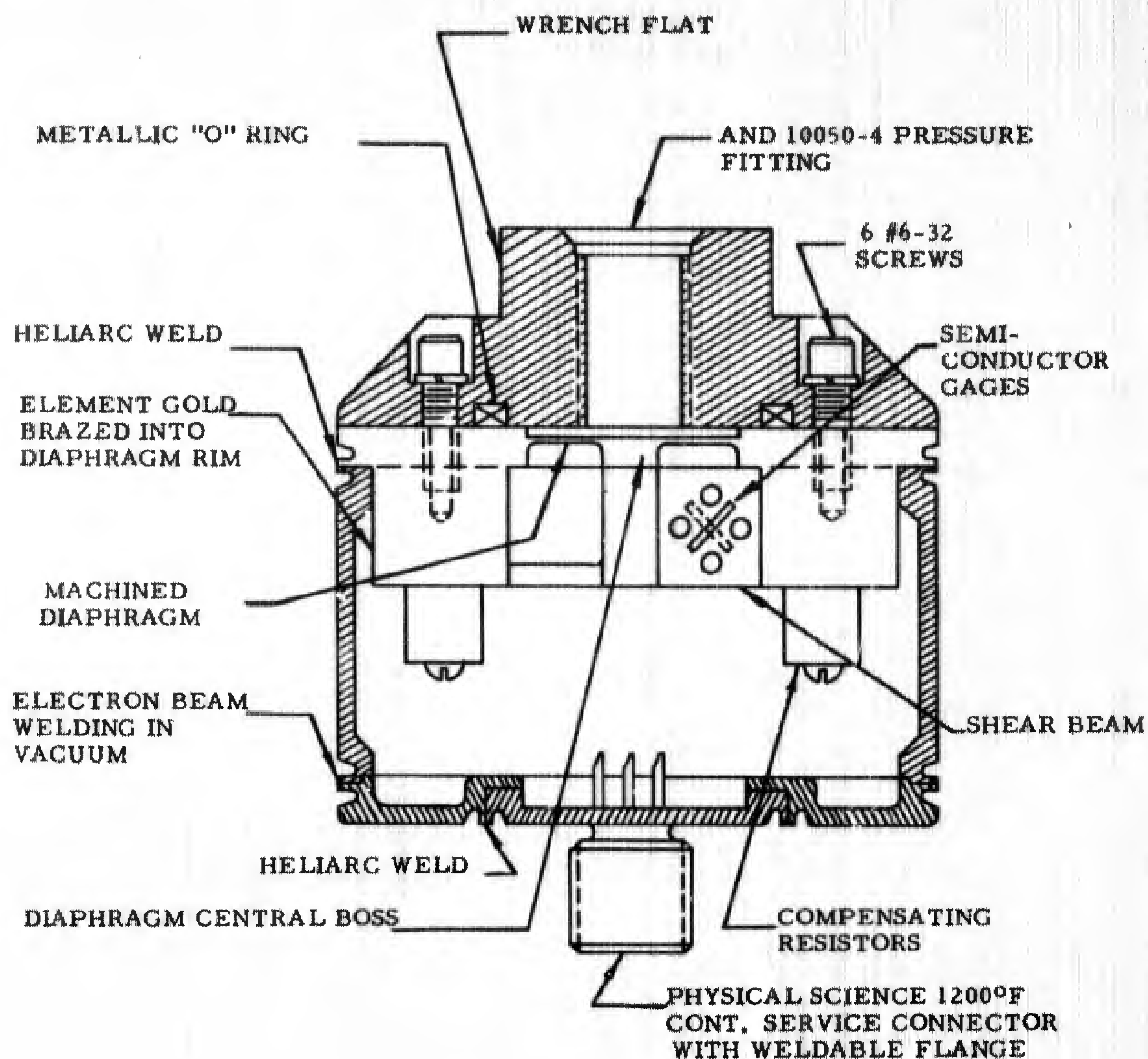

ACTUAL SIZE IS 2" DIA. x 2" LONG
SCALE: 2 x SIZE

ASSEMBLY FOR SHEAR BEAM TRANSDUCER

FIGURE 12

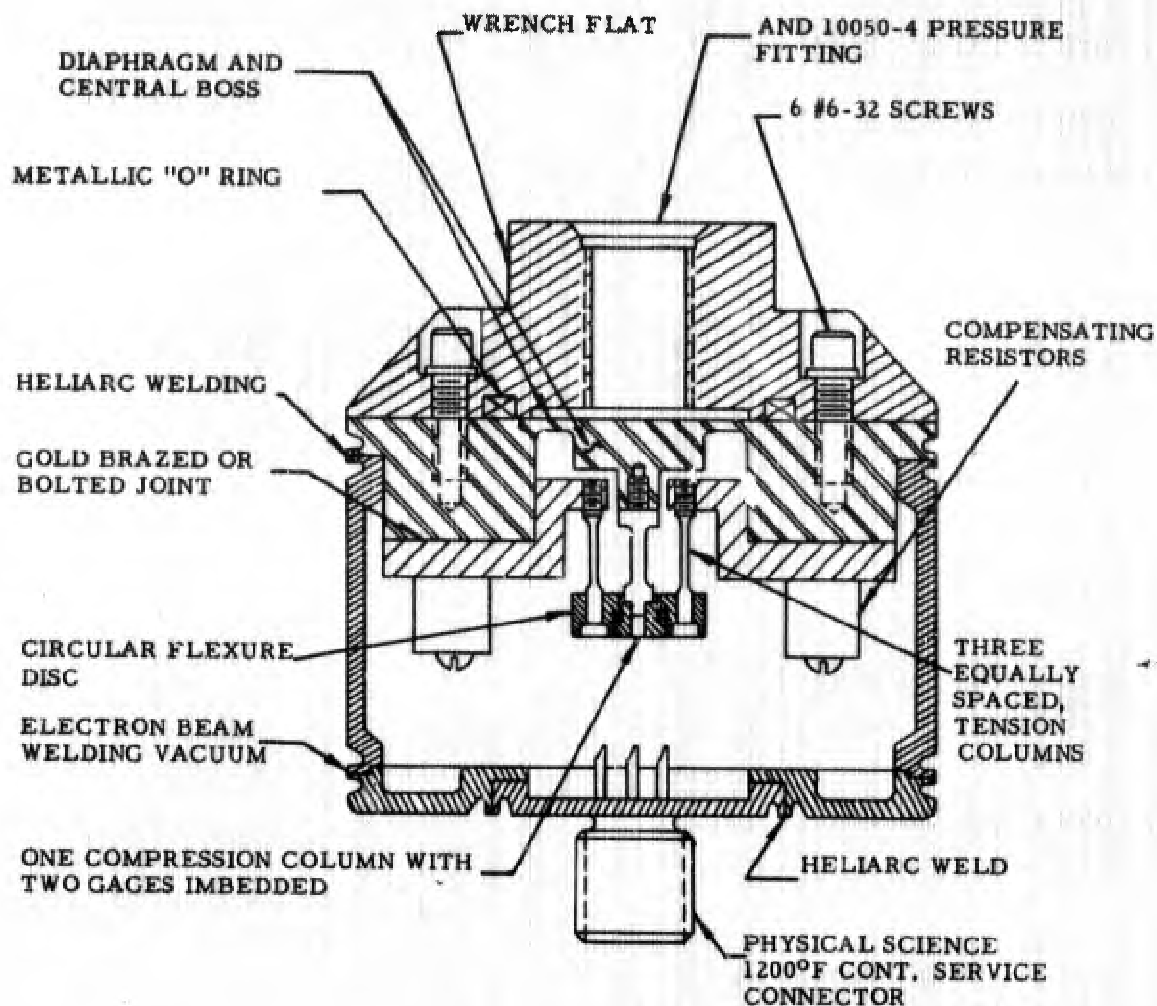

ACTUAL SIZE: 2" DIA. x 2" LONG
SCALE: 2:1

IMBEDDED GAGE TYPE PRESSURE TRANSDUCER ASSEMBLY

FIGURE 13

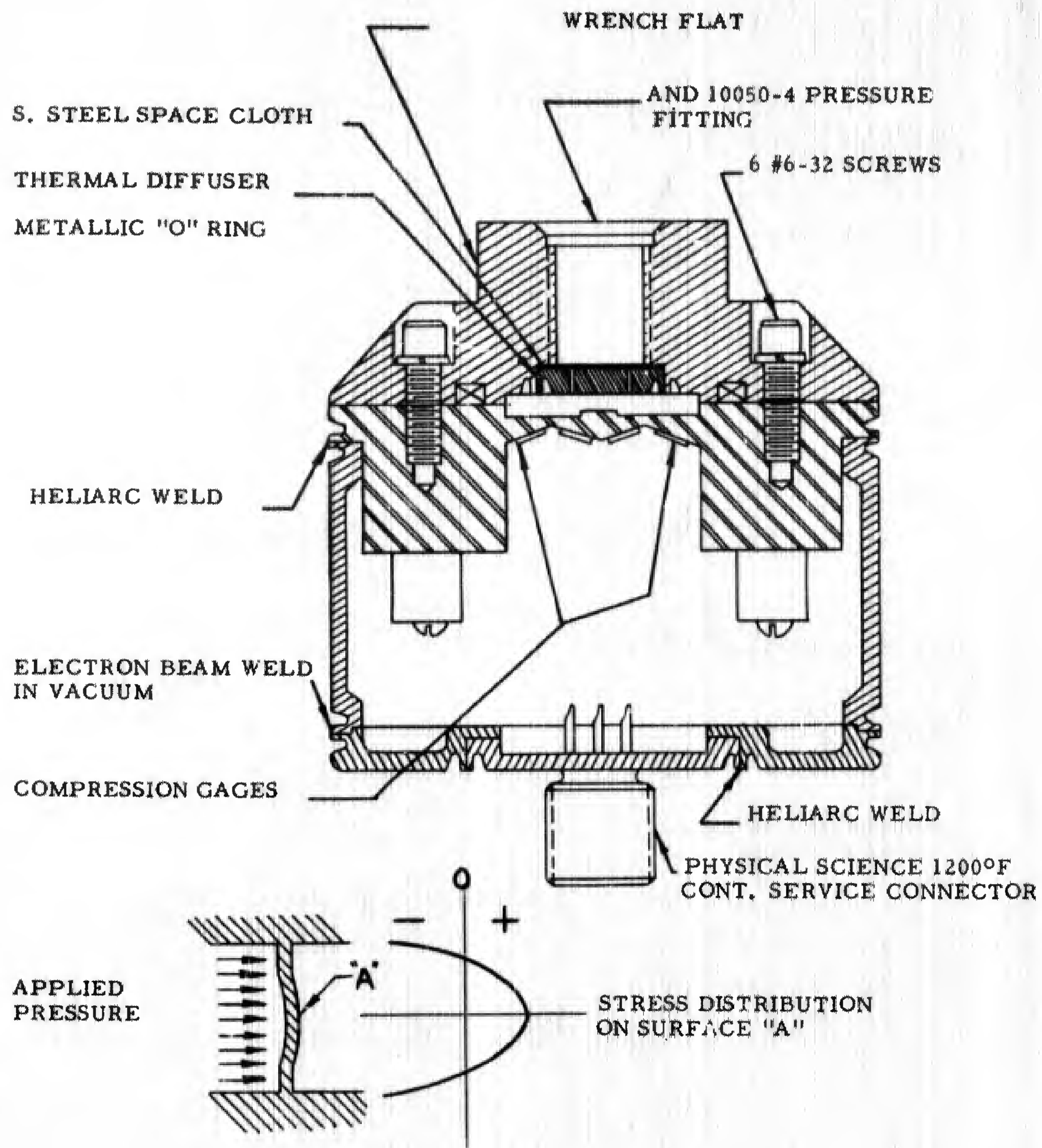

GAGED DIAPHRAGM TRANSDUCER

FIGURE 14

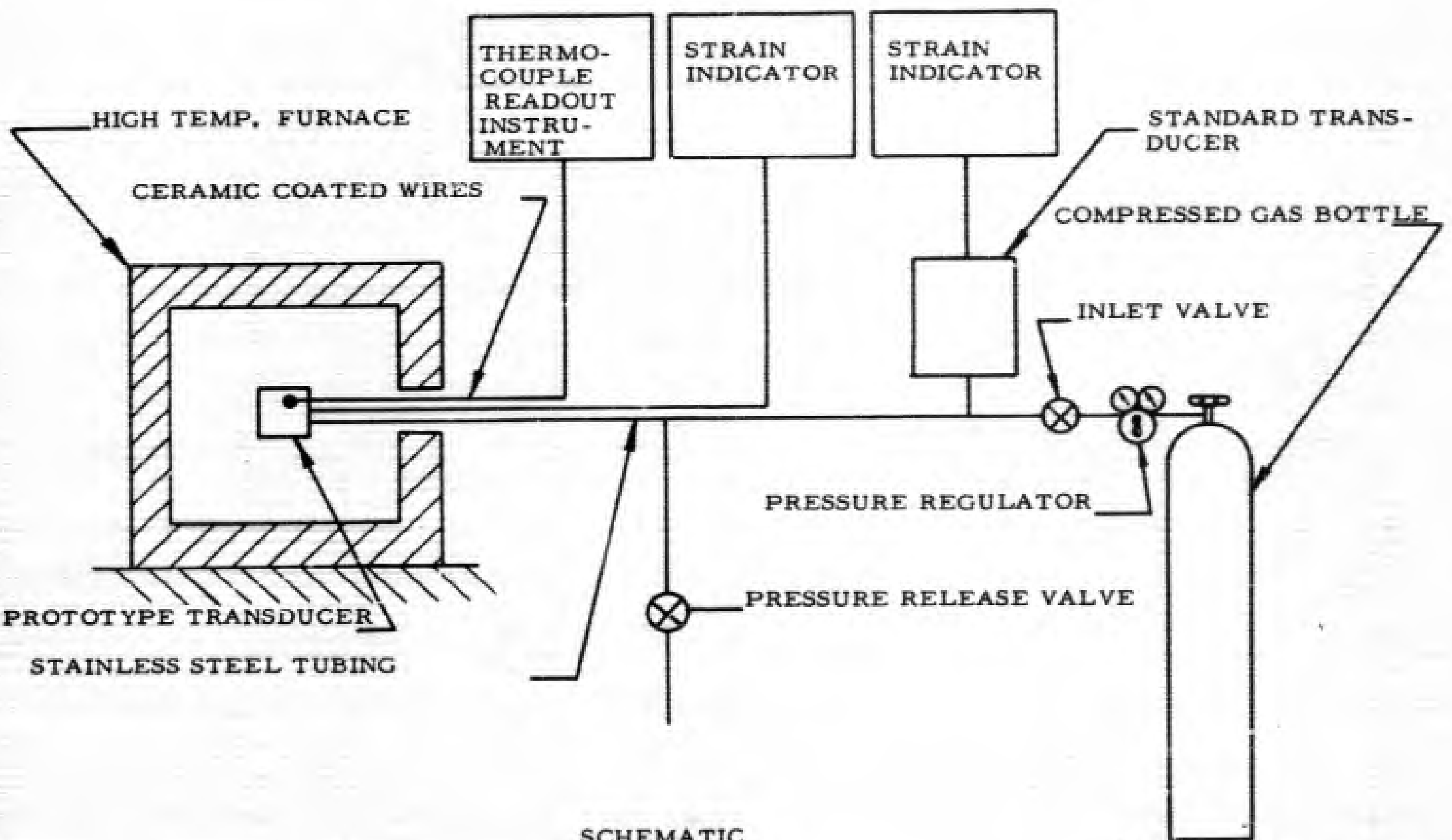

SCHEMATIC

FIGURE 15

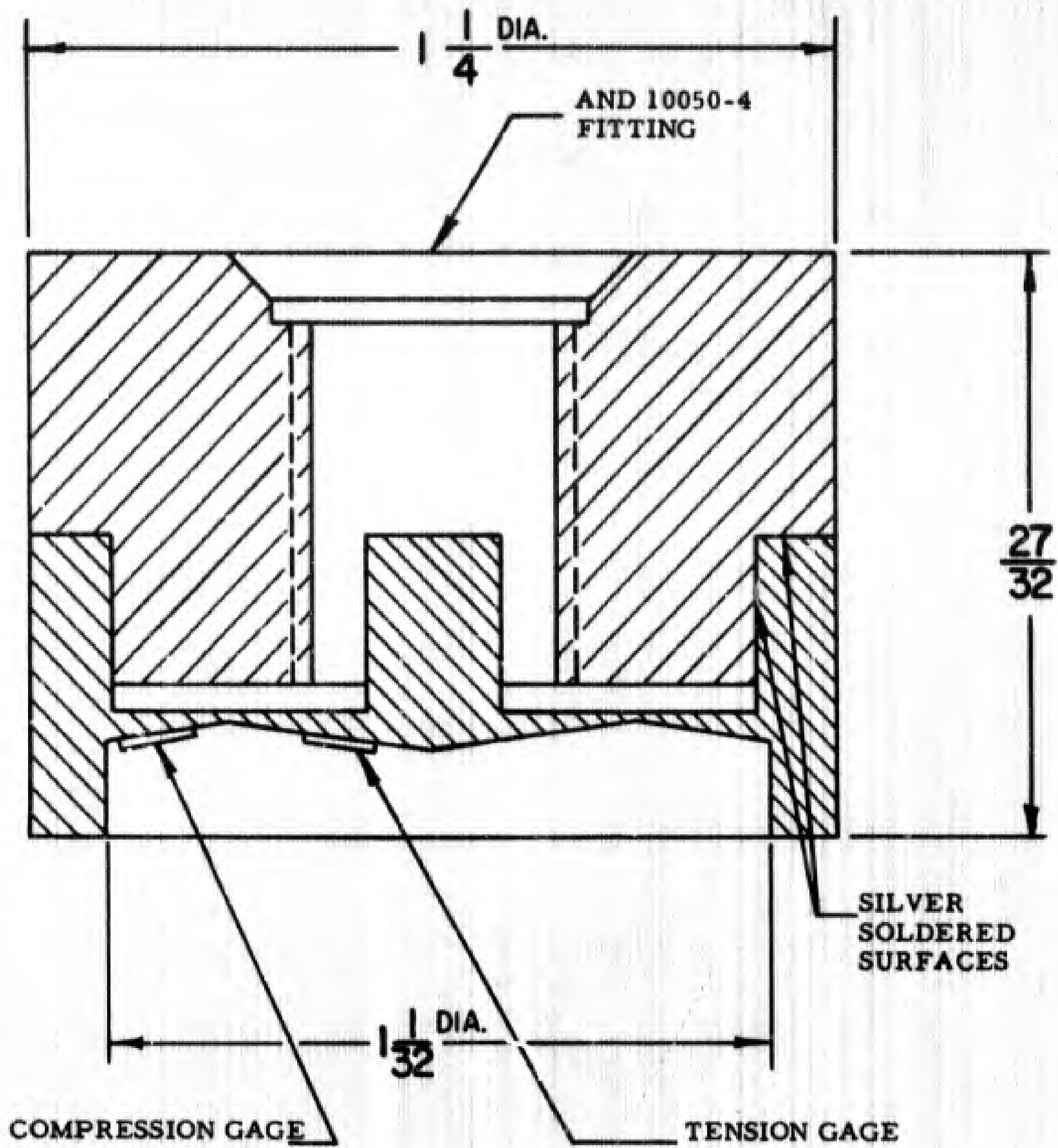

GAGED DIAPHRAGM TYPE TRANSDUCER CONSTRUCTION

FIGURE 16

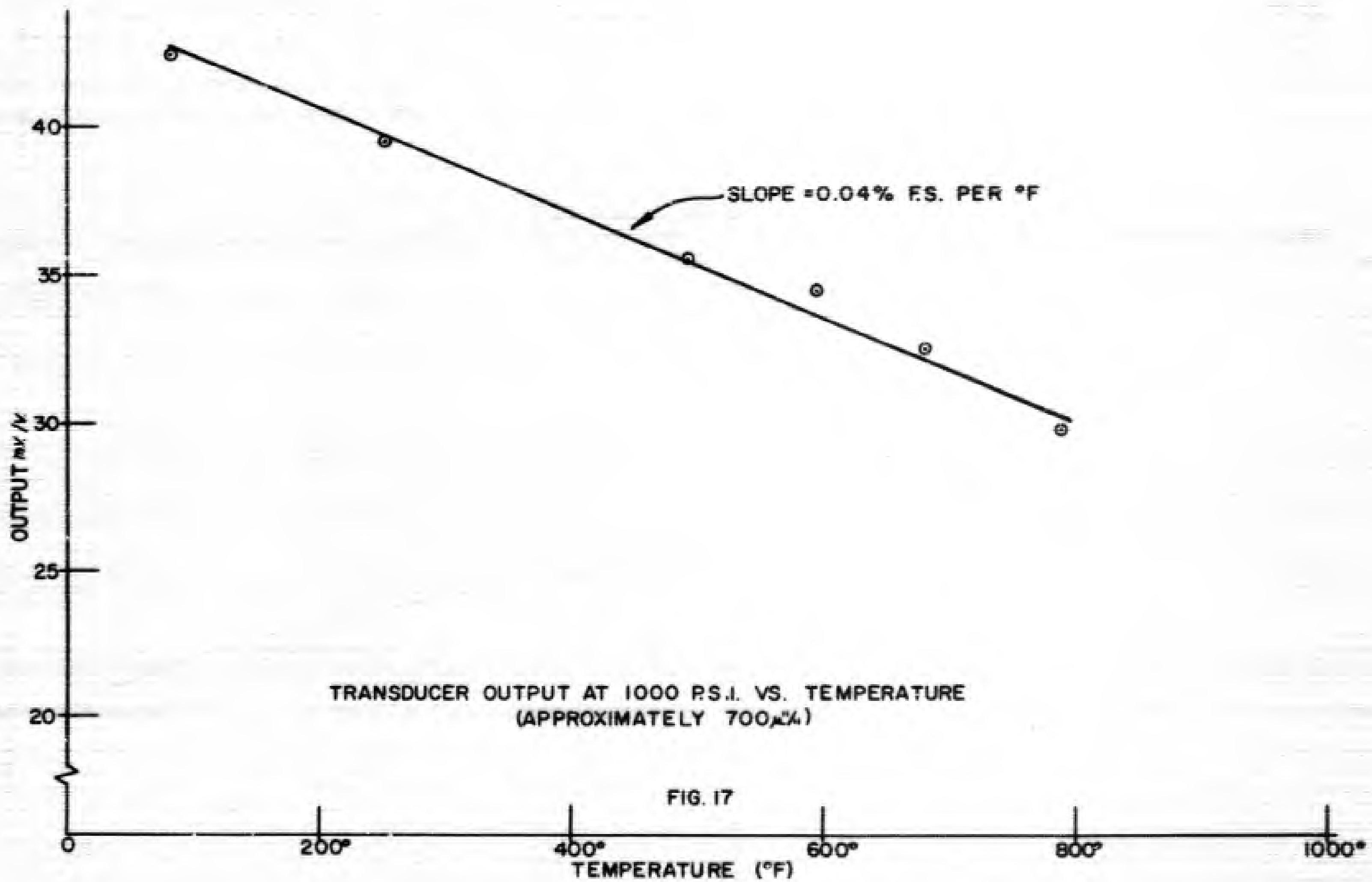

TRANSDUCER OUTPUT AT 1000 P.S.I. VS. TEMPERATURE
(APPROXIMATELY 700με)

FIG. 17

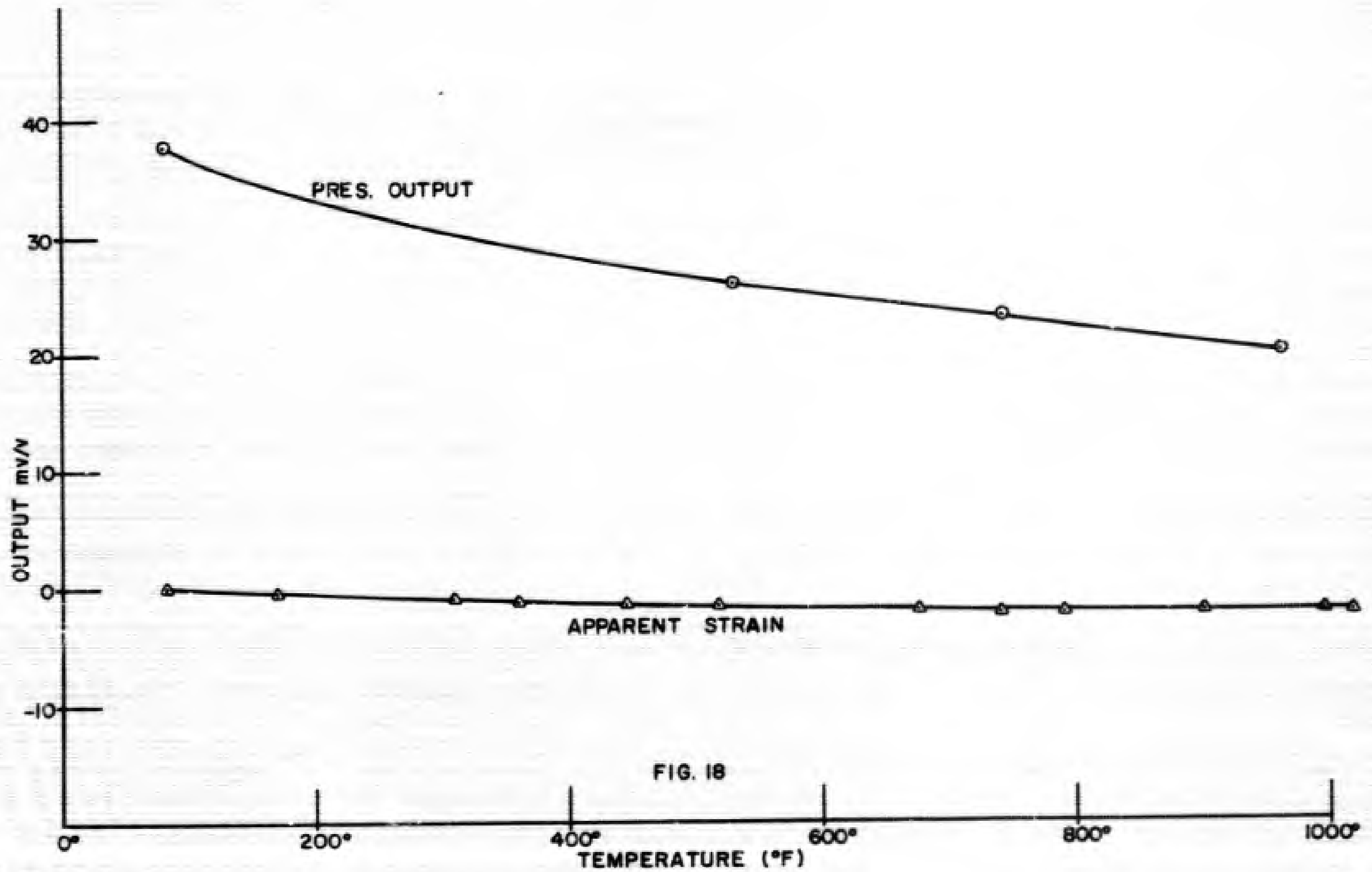

FIG. 18

TABLE 1

DIFFUSED SENSOR CHARACTERISTICS

Beam No.	Sensor A	Sensor B	Isolation of Sensors
1	279 ohms	276 ohms	2 megohms
2	342 ohms	323 ohms	1 meghoms
3	420 ohms	288 ohms	4 meghoms
4	342 ohms	323 ohms	4 meghoms
5	279 ohms	276 ohms	4 meghoms

TABLE 2

THERMAL GENERATION OF CARRIERS

T (°K)	T (°C)	Exp $(\frac{-14028}{T})$	n_i^2
300	27	4.93×10^{-21}	2.0×10^{20}
500	227	6.78×10^{-13}	1.3×10^{29}
700	427	1.98×10^{-9}	1.0×10^{33}
800	527	2.44×10^{-8}	1.9×10^{34}
1000	727	8.07×10^{-7}	1.2×10^{33}

TABLE 3

TEMPERATURE LIMITATION FOR EXTRINSIC BEHAVIOR

Resistivity	Impurity Concentration	Temperature
0.01 ohm-cm	1.1×10^{19} cm^{-3}	620°C (Fig. 6)
0.03 ohm-cm	2.9×10^{18} cm^{-3}	500°C (Fig. 7)
0.1 ohm-cm	5.0×10^{17}	400°C (Fig. 8)

TABLE 4

PRESTRAIN IN GAGES BONDED TO CERAMIC MATERIALS

Aluminum Oxide						
Test Temp. °F	78	233	476	686	942	1036
Unbonded Res. Ω	51.5	54.5*	65.9*	78.4*	95.0*	101.5*
Bonded Res. Ω	50.9	56.0	67.0	79.8	97.9	104.7
Chg. in Res. Ω	-.6	+1.5	+1.1	+1.4	+2.9	+3.2
Thermally ind. strain μ"/"	-101	+254	+201.5	+254	511	600
Cordierite						
Test Temp. °F	78	230	475	710	985	
Unbonded Res. Ω	52.5	55.8*	66.9*	81.5*	100.0*	
Bonded Res. Ω	50.2	56.6	67.4	83.6	98.2	
Chg. in Res. Ω	-2.3	+.8	+.5	+2.1	-1.8	
Thermally ind. strain μ"/"	-380	+139	+91	+369	-188.5	
Steatite						
Test Temp. °F	80	231	535	756	1015	
Unbonded Res. Ω	54.2	57.4*	72.6*	87.4*	106.4*	
Bonded Res. Ω	53.2	57.1	72.8	87.2	104.2	
Chg. in Res. Ω	-1.0	-.3	+.2	-.2	-2.2	
Thermally ind. strain μ"/"	-160	-54.1	+35.5	-34.6	-390	
*Extrapolated data						

TABLE 5

GAGE AND ISOLATION RESISTANCES AT VARIOUS TEMPERATURES

Test Temperature	Gage Resistance	Leakage to Ground
80°F	64.7	Infinite
148°F	62.6	"
250°F	62.2	"
400°F	64.8	"
600°F	73.9	2K megohms
700°F	81.2	30 megohms

TABLE 6

PRESTRAIN IN GAGES BONDED TO TUNGSTEN ALLOYS

Tungsten Alloy 955						
Test Temp. °F	77	225	510	724	1004	70
Unbonded Res. Ω	48.7	51.6	64.1	78.7	94.3	48.7
Bonded Res. Ω	50.1	54.9	68.3	80.7	100.1	49.7
Chg. in Res. Ω	+1.4	+3.3	4.2	2	5.8	1
Thermally ind. strain μ"/"	243	590	780	370	1068	175

Tungsten Alloy 982						
Test Temp. °F	78	225	500	715	1029	75
Unbonded Res. Ω	49.5	52.5	64.8	76.4	96.5	49.5
Bonded Res. Ω	50.0	53.6	65.1	76.6	100.6	48.8
Chg. in Res. Ω	.5	1.1	.3	.2	4.1	-.7
Thermally ind. strain μ"/"	87	201	57/5	38.7	785	-123

TABLE 7

BEHAVIOR OF TUNGSTEN BEAM AT VARIOUS TEMPERATURES

Temperature (°F)	Maximum Non-Linearity	Zero Shift (MV/V)	Leakage (Megohms)
72	.22%	-.04	10,000
241	3.0 %	+.01	10,000
501	.15%	+.04	5,000
698	.22%	0	
802	.43%	0	4,000
900	.33%	-.02	200
995	.42%	-.06	8

TABLE 8

BEHAVIOR OF NISPAN C BEAM AT VARIOUS TEMPERATURES

Temperature (°F)	Apparent Strain MV/V	Force Output (MV/V)	Leakage (Megohms)
80	-40.74	21.34	10K
251	-18.07	19.38	10K
495	-10.74	15.60	8K
600°F	Gages cracked		

TABLE 9

PRESTRAIN IN GAGES BONDED TO NISPAN C BEAM

First Gage	80°F	251°F	495°F
Unbonded gage resistance (ohms)	61.2	65.7*	79.6*
After bonding (ohms)	60.2	63.1	85.5
Change of resistance (ohms)	-1.0	-2.6	+5.9
Thermally induced strain $\mu''/''$	-160	-380	+660
Second Gage	**80°F**	**251°F**	**495°F**
Unbonded gage resistance (ohms)	67.6	72.7*	88.0*
After bonding (ohms)	72.7	71.6	89.6
Change of resistance (ohms)	+5.1	-.9	+1.6
Thermally induced strain $\mu''/''$	+800	-110	+160

*Extrapolated data from Fig. 6

TABLE 10

BEHAVIOR OF SILICON BEAM AT VARIOUS TEMPERATURES

Temperature °F	Apparent Strain (MV/V)	Force Output (MV/V)	Leakage (ohms)
84	-.29	21.54	900K
250	-8.26	17.93	200K
507	-18.72	13.22	10K
755	-31.23	8.80	750

TABLE 11

BEHAVIOR OF CERAMIC BEAMS AT VARIOUS TEMPERATURES

Lucalox Beam

Temperature °F	Apparent Strain (MV/V)	Output (MV/V)	Leakage (Megohms)
84	-8.27	6.83	Inf.
252	-2.17	6.67	10K
504	-10.40	6.13	10K
750	-6.49	5.30	7K
80	-5.87		

Gages became very noisy at temperature higher than 750°F.

Advac Beam

Temperature °F	Apparent Strain (MV/V)	Output (MV/V)	Leakage (Megohms)
80	-5.20	6.64	Inf.
234	+7.05	5.98	10K
508	+63.17	5.00	2K
601	+66.12	4.30	

Continuous drift at 600°F.

Duramic Beam

Temperature °F	Apparent Strain (MV/V)	Output (MV/V	Leakage (Megohms)
74	-2.70	30.93	Inf.
227	+1.26	26.84	10K
487	+13.26	21.19	2K

Gages became noisy at higher temperatures.

TABLE 12

OUTPUT CHARACTERISTICS OF STANDARD PRESSURE TRANSDUCER

Output in millivolts of the pressure transducer used as pressure standard at calibration points.		
Applied Pressure (psig)	1st Run	2nd and 3rd Run
0	0	0
200	51.79	51.79
400	103.59	103.59
600	155.39	155.39
800	207.19	207.19
1000	258.97	258.97
800	207.25	207.19
600	155.51	155.39
400	103.72	103.59
200	51.89	51.79
0	0.01	0.00
Linearity	.005%	.005%
Hysteresis	.05%	0

The results of the second and third run were used as pressure standards.

TABLE 13

PRESSURE LOADING AT HIGH TEMPERATURES OF FIRST PROTOTYPE

Actual data of gaged diaphragm transducer before regaging. Excited with 3 volts DC.

Applied Pressure (psig)	Output in MV			
	Room Temp.	253°F	273°F	430°F
0	0	0	0	0
200	22.18	20.64	20.70	21.64
400	44.24	41.80	41.68	43.68
600	66.66	62.82	62.72	65.70
800	89.08	83.94	83.78	87.90
1000	111.36	105.20	105.00	
800	89.92	85.06	85.06	gage lead failed
600	67.84	64.38	64.42	
400	45.44	42.34	43.40	
200	22.98	22.02	22.14	
0	.34	0.48	0.68	

Actual data of gage diaphragm transducer after regaging. Excited with 3 volts DC.

Applied Pressure (psig)	80°F	252°F	492°F	595°F	680°F	787°F
0	0	0	0	0	0	0
200	25.32	23.50	20.68	20.02	18.92	17.55
400	50.88	47.34	41.64	40.30	37.88	35.40
600	76.38	71.14	62.72	60.68	57.10	53.25
800	101.76	94.84	83.84	81.24	76.40	71.24
1000	127.06	118.74	106.50	103.20	97.20	89.12
800	102.68	96.08	85.40	82.62	77.64	72.18
600	77.78	72.76	64.72	62.52	58.74	54.64
400	52.34	48.98	43.74	42.00	39.54	36.62
200	26.52	24.90	22.32	21.40	20.14	18.50
0	0.48	.56	.84	.48	.18	0

At 900°F, the transducer was functioning properly, however, no data was taken. At 1000°F gage lead failed.

TABLE 14

PRESSURE LOADING AT ROOM TEMPERATURE OF SECOND PROTOTYPE

Applied Pressure (psi)	Output (MV/V)	Theroretical Straight Line Output (MV/V)	Error (MV/V)	Non-Linearity (% F.S.)
0	0	0	0	0
200	6.800	6.906	-0.008	-0.02
400	13.800	13.816	-0.016	-0.05
600	20.704	20.724	-0.020	-0.06
800	27.616	27.632	-0.016	-0.05
1000	34.540	34.540	0	0
800	27.736	27.632	+0.104	
600	20.872	20.724	+0.148	
400	13.992	13.816	+0.176	
200	7.000	6.908	+0.092	
0	0.880	0	+0.880	

Test Temperature 80°F

Note: Data represents the results after exercising 3 times.
Initial zero shift is approximately 1 MV/V.
Alloy #955K gaged with Pyroceram.

TABLE 15
PRESSURE LOADING AT 227°F OF SECOND PROTOTYPE

Applied Pressure (psi)	Output (MV/V)	Theoretical Straight Line Output (MV/V)	Error (MV/V)	Non-Linearity (% F.S.)
0	0	0	0	0
200	6.124	6.182	-0.058	-0.19
400	12.272	12.365	-0.093	-0.30
600	18.432	18.547	-0.115	-0.37
800	24.620	24.730	-0.110	-0.36
1000	30.912	30.912	0	0
800	24.876	24.730	0.146	
600	18.764	18.547	0.217	
400	12.624	12.365	0.259	
200	6.320	6.182	0.138	
0	0.136	0	0.136	
0 (1 min.)	0.100	0	0.100	

Test Temperature 227°F

Note: During the initial load, zero shifted in excess of
4 MV/V due to creep at load.
Alloy #955K gaged with Pyroceram.

TABLE 16

PRESSURE LOADING AT 548°F OF SECOND PROTOTYPE

Applied Pressure (psi)	Output (MV/V)	Theoretical Straight Line Output (MV/V)	Error (MV/V)	Non-Linearity (% F.S.)
0	0	0	0	0
200	4.816	4.888	-0.062	-0.25
400	9.644	9.776	-0.132	-0.54
600	14.488	14.664	-0.176	-0.72
800	19.408	19.552	-0.144	-0.59
1000	24.440	24.440	0	0
800	19.848	19.552	+0.296	
600	15.168	14.664	+0.504	
400	10.480	9.776	+0.704	
200	5.644	4.888	+0.756	
0	0.800	0	+0.800	

Test Temperature 548°F

Note: Data represents the results after exercising 3 times to full scale pressure.
Alloy #955K gaged with Pyroceram.

TABLE 17

PRESSURE LOADING AT 235°F OF SECOND PROTOTYPE

Applied Pressure (psi)	Output (MV/V	Theoretical Straight Line Output (MV/V)	Error (MV/V)	Non-Linearity (% F.S.)
0	0	0	0	0
200	5.928	5.916	+0.012	+0.04
400	11.868	11.832	+0.036	+0.12
600	17.760	17.748	+0.012	+0.04
800	23.644	23.664	-0.020	-0.07
1000	29.580	29.580	0	0
800	23.752	23.664	+0.088	
600	17.880	17.748	+0.132	
400	11.968	11.832	+0.136	
200	5.992	5.916	+0.016	
0	0	0	0	

Test Temperature 235°F

Note: Data represents the results after exercising 3 times to full scale pressure. Initial zero shift is 0.12 MV/V.
Alloy#955K gaged with Pyroceram.

TABLE 18

PRESSURE LOADING AT VARIOUS
TEMPERATURES OF THIRD PROTOTYPE

Applied Pressure (psig)	Output in MV/V at Various Temperatures				
	80°F	530°F	740°F	958°F	74°F
0	0	0	0	0	0
200	7.56	5.14	4.46	3.92	7.98
400	15.12	10.38	9.06	7.83	15.92
600	22.60	15.64	13.78	11.71	23.74
800	30.10	20.52	18.32	15.82	31.59
1000	37.54	25.72	22.86	19.89	39.41
800	30.06	21.14	18.38	16.18	31.55
600	22.54	15.78	13.87	12.35	23.67
400	15.06	10.52	9.23	8.47	15.81
200	7.50	5.26	4.55	4.72	7.90
0	0	.06	0.02	0.84	0
Linearity, % F.S.	+.19	+0.81	-.25	-1.6	+.40
Hysteresis and Zero Shift, % F.S.	+.12	+0.56	+.90	+11.0	.13

Data represents results after exercising three times to full scale pressure.

Unclassified
Security Classification

DOCUMENT CONTROL DATA - R&D

(Security classification of title, body of abstract and indexing annotation must be entered when the overall report is classified)

1. ORIGINATING ACTIVITY (Corporate author) Schaevitz-Bytrex, Incorporated 223 Crescent Street Waltham, Massachusetts	2a. REPORT SECURITY CLASSIFICATION Unclassified 2b. GROUP

3. REPORT TITLE
"COMPENSATION TECHNIQUES INVESTIGATION FOR HIGH TEMPERATURE OPERATION OF P-SILICON PRESSURE TRANSDUCERS"

4. DESCRIPTIVE NOTES (Type of report and inclusive dates)
Final Report, 15 July 1964 - 29 March 1965

5. AUTHOR(S) (Last name, first name, initial)
Yuen, Frank L.

6. REPORT DATE	7a. TOTAL NO. OF PAGES	7b. NO. OF REFS
November 1965	58	None

8a. CONTRACT OR GRANT NO. AF33(615)-1865	9a. ORIGINATOR'S REPORT NUMBER(S)
b. PROJECT NO. 8224	Job Nr. 1775
c. Task Nr. 822403	9b. OTHER REPORT NO(S) (Any other numbers that may be assigned this report)
d.	AFFDL-TR-65-130

10. AVAILABILITY/LIMITATION NOTICES
Qualified requesters may obtain copies of this report from DDC. Foreign announcement and dissemination of this report by DDC is not authorized. DDC releast to CFSTI is not authorized.

11. SUPPLEMENTARY NOTES	12. SPONSORING MILITARY ACTIVITY
	AF Flight Dynamics Laboratory, RTD Flight Control Division (FDCL) Wright-Patterson AFB, Ohio

13. ABSTRACT

Theoretical study and experimental work indicate that a p-n junction type diffused semiconductor sensor is not feasible for high temperature operation above 600°F or 700°F. The generation of electron hole pairs destroys the isolation property of the p-n junction. Consequently, emphasis was shifted to work on the development of a semiconductor pressure transducer with bonded strain sensors. The bulk resistivity of the silicon sensor was established together with the technique of effecting a high temperature ohmic contact. A broad evaluation of the substrate materials was made before the final selection of a special tungsten allow stock for actual transducer fabrication. Prototype transducers were built and tested at temperatures above 1000°F. The data from temperature compensation experiments showed that the techniques and choice of materials will make high temperature pressure transducers which satisfy most of the requirements of the Statement of Work for this contract.

DD FORM 1 JAN 64 1473

Unclassified
Security Classification

Security Classification

14. KEY WORDS	LINK A		LINK B		LINK C	
	ROLE	WT	ROLE	WT	ROLE	WT

INSTRUCTIONS

1. ORIGINATING ACTIVITY: Enter the name and address of the contractor, subcontractor, grantee, Department of Defense activity or other organization *(corporate author)* issuing the report.

2a. REPORT SECURITY CLASSIFICATION: Enter the overall security classification of the report. Indicate whether "Restricted Data" is included. Marking is to be in accordance with appropriate security regulations.

2b. GROUP: Automatic downgrading is specified in DoD Directive 5200.10 and Armed Forces Industrial Manual. Enter the group number. Also, when applicable, show that optional markings have been used for Group 3 and Group 4 as authorized.

3. REPORT TITLE: Enter the complete report title in all capital letters. Titles in all cases should be unclassified. If a meaningful title cannot be selected without classification, show title classification in all capitals in parenthesis immediately following the title.

4. DESCRIPTIVE NOTES: If appropriate, enter the type of report, e.g., interim, progress, summary, annual, or final. Give the inclusive dates when a specific reporting period is covered.

5. AUTHOR(S): Enter the name(s) of author(s) as shown on or in the report. Enter last name, first name, middle initial. If military, show rank and branch of service. The name of the principal author is an absolute minimum requirement.

6. REPORT DATE: Enter the date of the report as day, month, year; or month, year. If more than one date appears on the report, use date of publication.

7a. TOTAL NUMBER OF PAGES: The total page count should follow normal pagination procedures, i.e., enter the number of pages containing information.

7b. NUMBER OF REFERENCES: Enter the total number of references cited in the report.

8a. CONTRACT OR GRANT NUMBER: If appropriate, enter the applicable number of the contract or grant under which the report was written.

8b, 8c, & 8d. PROJECT NUMBER: Enter the appropriate military department identification, such as project number, subproject number, system numbers, task number, etc.

9a. ORIGINATOR'S REPORT NUMBER(S): Enter the official report number by which the document will be identified and controlled by the originating activity. This number must be unique to this report.

9b. OTHER REPORT NUMBER(S): If the report has been assigned any other report numbers *(either by the originator or by the sponsor)*, also enter this number(s).

10. AVAILABILITY/LIMITATION NOTICES: Enter any limitations on further dissemination of the report, other than those imposed by security classification, using standard statements such as:

(1) "Qualified requesters may obtain copies of this report from DDC."

(2) "Foreign announcement and dissemination of this report by DDC is not authorized."

(3) "U. S. Government agencies may obtain copies of this report directly from DDC. Other qualified DDC users shall request through
____."

(4) "U. S. military agencies may obtain copies of this report directly from DDC. Other qualified users shall request through
____."

(5) "All distribution of this report is controlled. Qualified DDC users shall request through
____."

If the report has been furnished to the Office of Technical Services, Department of Commerce, for sale to the public, indicate this fact and enter the price, if known.

11. SUPPLEMENTARY NOTES: Use for additional explanatory notes.

12. SPONSORING MILITARY ACTIVITY: Enter the name of the departmental project office or laboratory sponsoring *(paying for)* the research and development. Include address.

13. ABSTRACT: Enter an abstract giving a brief and factual summary of the document indicative of the report, even though it may also appear elsewhere in the body of the technical report. If additional space is required, a continuation sheet shall be attached.

It is highly desirable that the abstract of classified reports be unclassified. Each paragraph of the abstract shall end with an indication of the military security classification of the information in the paragraph, represented as *(TS)*, *(S)*, *(C)*, or *(U)*.

There is no limitation on the length of the abstract. However, the suggested length is from 150 to 225 words.

14. KEY WORDS: Key words are technically meaningful terms or short phrases that characterize a report and may be used as index entries for cataloging the report. Key words must be selected so that no security classification is required. Identifiers, such as equipment model designation, trade name, military project code name, geographic location, may be used as key words but will be followed by an indication of technical context. The assignment of links, rules, and weights is optional.

Security Classification